Results and Discussions

CHAPTER NO 4: RESULTS AND DISCUSSION

Part A- Evaluation of anti-proliferative and pro-apoptotic efficacy of phenolic fraction of *Etlingera linguiformis.*

In this section we are presenting our findings on efficacy of free phenolics and bound phenolics extracted from *Etlingera linguiformis* (CAN). The data generated using standard methods that are commonly used in such studies using *in vitro* and *in vivo* models.

4.1. Cytotoxicity Assay against Human RBCs and PBMCs

To check the toxicity of the selected plant extract we have used the membrane stability activity on human RBCs against Triton-X 100 induced haemolysis and viability of human PBMCs using MTT based method.

The CAN phenolic extract shows protective role against Triton-X 100 induced haemolysis with respect to the +ve and –ve control (Figure 4.1). The activity of the plant extract was compared with ascorbic acid. On the other hand, the cell viability was observed at 24 h when the human PBMCs were exposed to either the CAN free phenolic and CAN bound phenolic extract. Cell viability was shown to be higher than the control with rising concentration across all time periods of exposure (Figure 4.2), suggesting that CAN extract is not toxic to human RBCs and substantially stimulates proliferation in human PBMCs ($p \leq 0.001$).

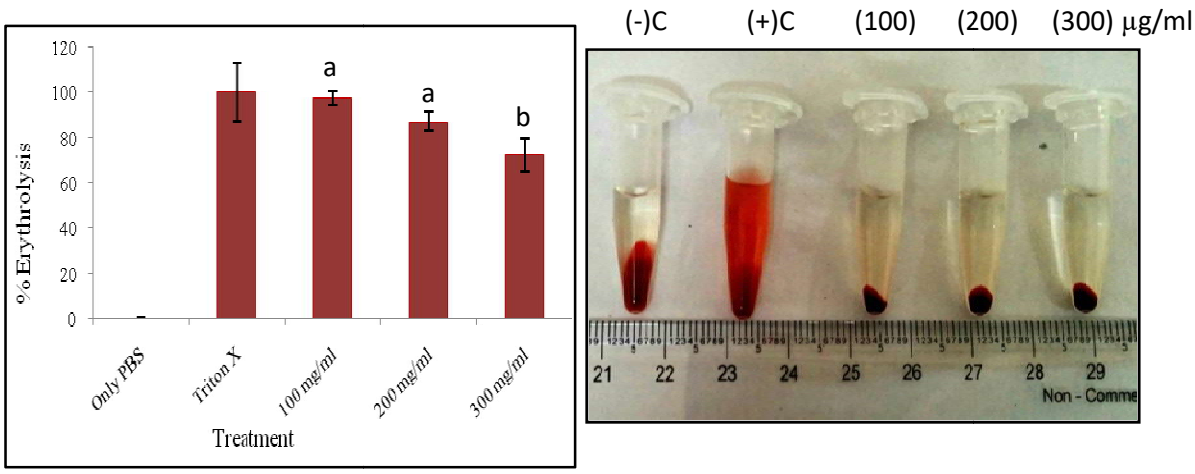

Figure 4.1: Effect of different concentration of CAN on % inhibition of Triton-X induced haemolysis of human erythrocytes incubated in PBS. Values were expressed as mean ± sem; n=3. Error bars represent standard deviation [a] Significantly different ($p \leq 0.001$) against untreated control. [b] Significantly different ($p \leq 0.01$) against

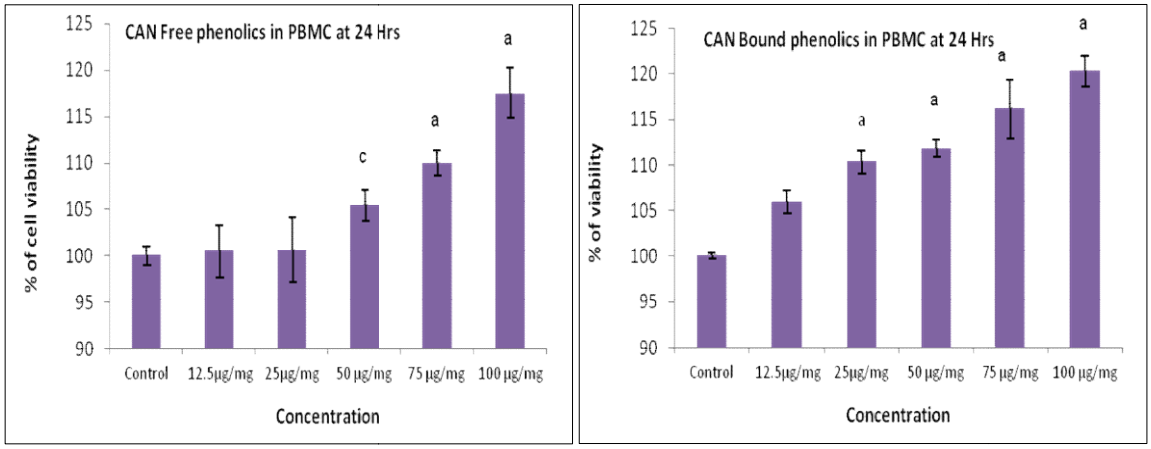

Figure 4.2: Cytotoxic effects of (a) CAN FP at 24 h and (b) CAN BP at 24 h, measured by MTT based method. Values were expressed as mean ± sem; n=3. Error bars represent standard deviation [a] Significantly different ($p \leq 0.001$) against untreated control. [b] Significantly different ($p \leq 0.01$) against untreated control.

4.2. Cytotoxicity effect of CAN free phenolic and CAN bound phenolic on human lung cancer cell lines

CAN free phenolic and CAN bound phenolic extracts were tested for their cytotoxicity on human lung cancer cell lines; A549, NCI-H522 and NCI-H23, using the MTT based method and trypan blue exclusion assay. For 24 and 48 hours, cells were treated to either the extracts at concentrations of 25, 50, 100 μg/ml, or the vehicle control, 0.1% DMSO.

The CAN free phenolic and CAN bound phenolic fraction shows inhibition of cell viability on human lung cancer cell lines at dose dependent manner after 24 and 48 hours of treatment. It also strongly limit the overall cell growth in a dose dependent manner in all three cell lines with noticeably reduced in IC50 values (Figure 4.3, 4.4, 4.5 and 4.6). The number of death cell substantially increases with respect to the dose and time of incubation with the phenolic fractions of CAN

The plant fractions shows selective cytotoxicity in cancer cell lines yet remain non toxic to normal human cells, suggesting the presence of specific photochemical in the plant extracts.

Exploration of such plant based active compound would enlighten the discovery of new anticancer therapeutics and reduce the cost and other limitations that tagged with conventional anticancer approach/module present today.

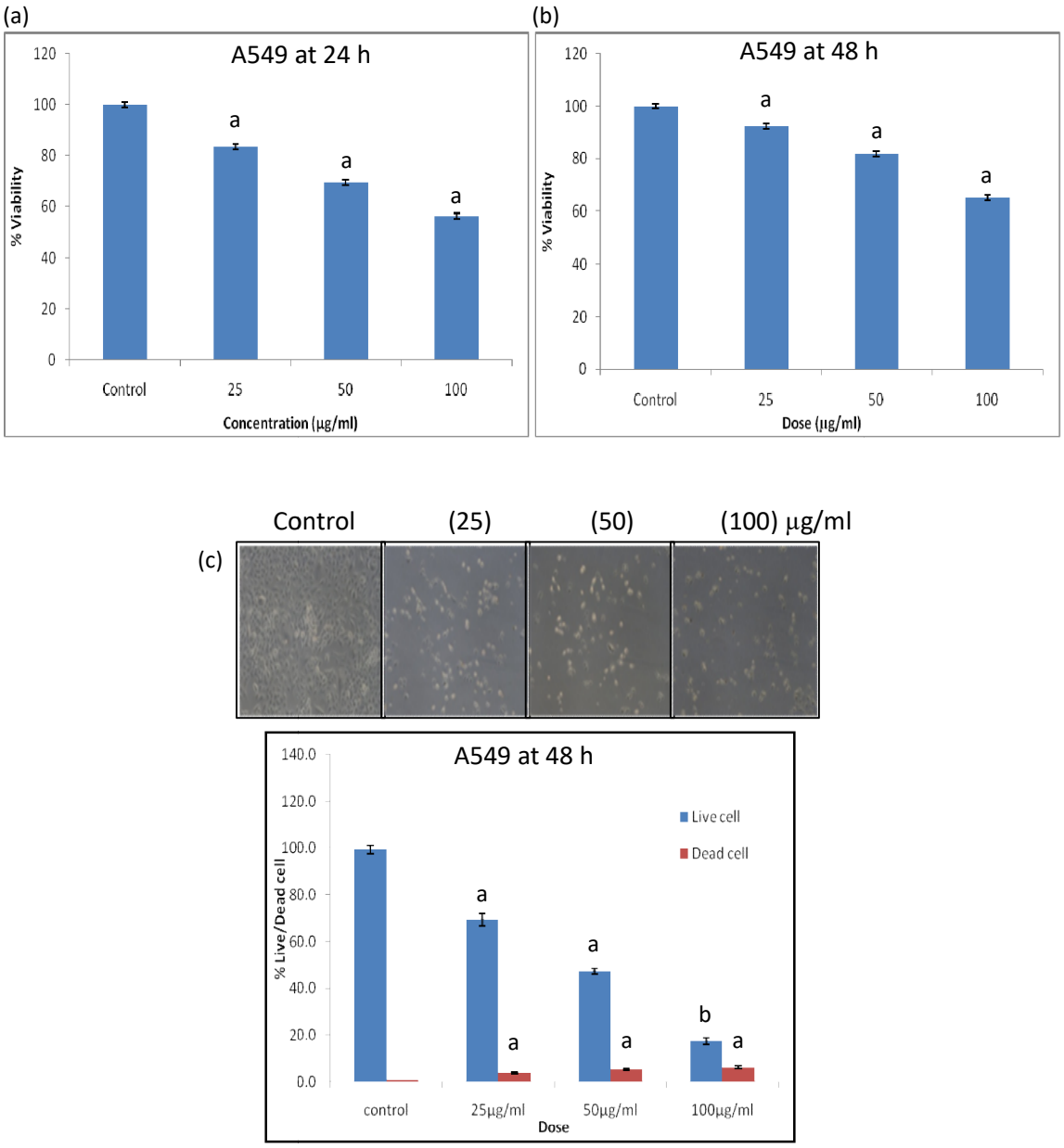

Figure 4.3: Cytotoxic effects of (a) CAN FP at 24 h and (b) CAN FP at 48 h against A549 cells, measured by MTT based method. (c) Cell counting assay of A549 cells against CAN FP measured by trypan blue dye exclusion method. The viability is calculated as % of control (100%) Values were expressed as mean ± sem; n=3. Error bars represent standard deviation [a] Significantly different ($p \leq 0.001$) against untreated control. [b] Significantly different ($p \leq 0.01$) against untreated control.

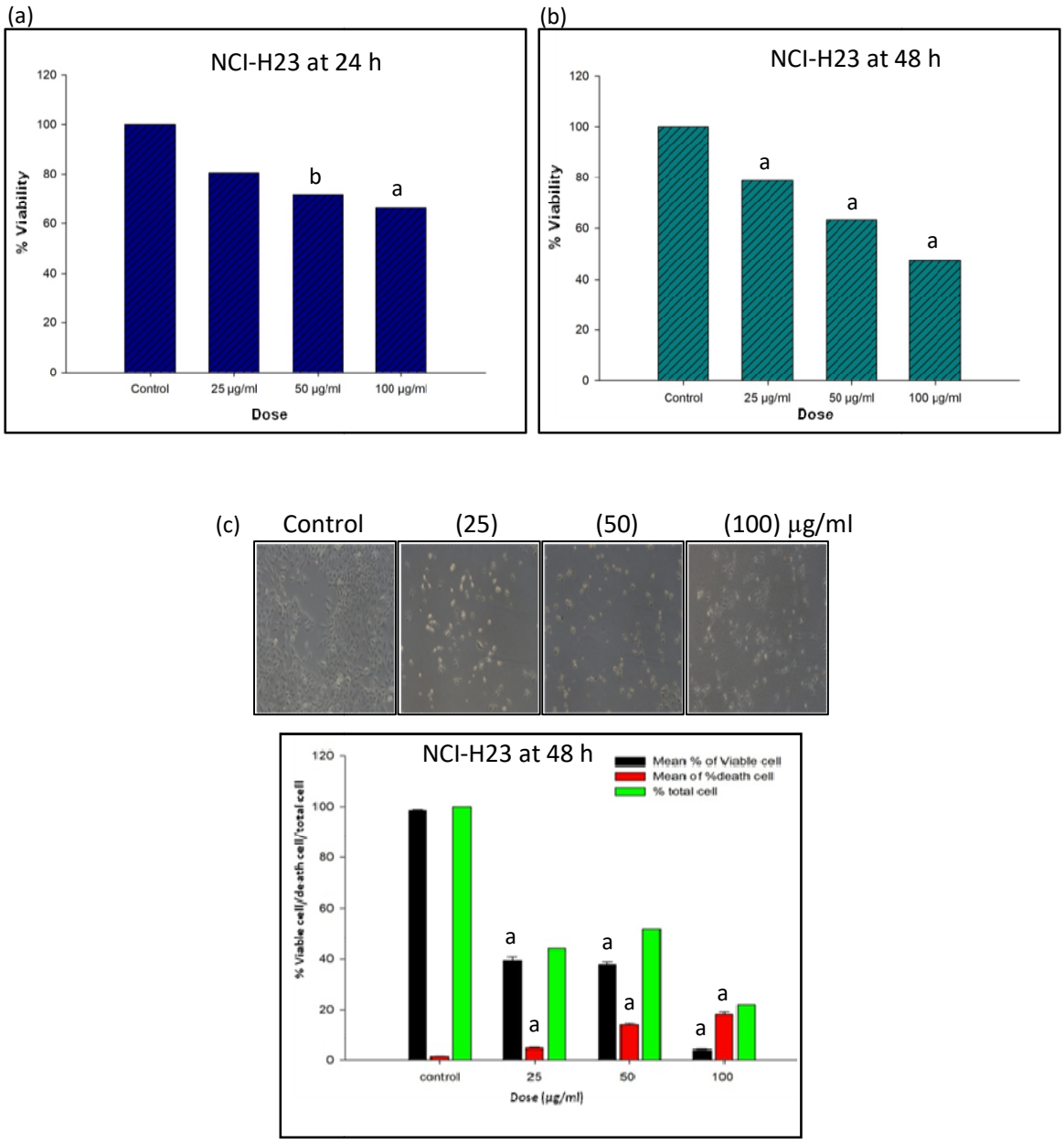

Figure 4.4: Cytotoxic effects of (a) CAN FP at 24 h and (b) CAN FP at 48 h against NCI-H23 cells, measured by MTT based method. (c) Cell counting assay of NCI-H23 cells against CAN FP measured by trypan blue dye exclusion method. The viability is calculated as % of control (100%) Values were expressed as mean ± sem; n=3. Error bars represent standard deviation [a] Significantly different ($p \leq 0.001$) against untreated control. [b] Significantly different ($p \leq 0.01$) against untreated control.

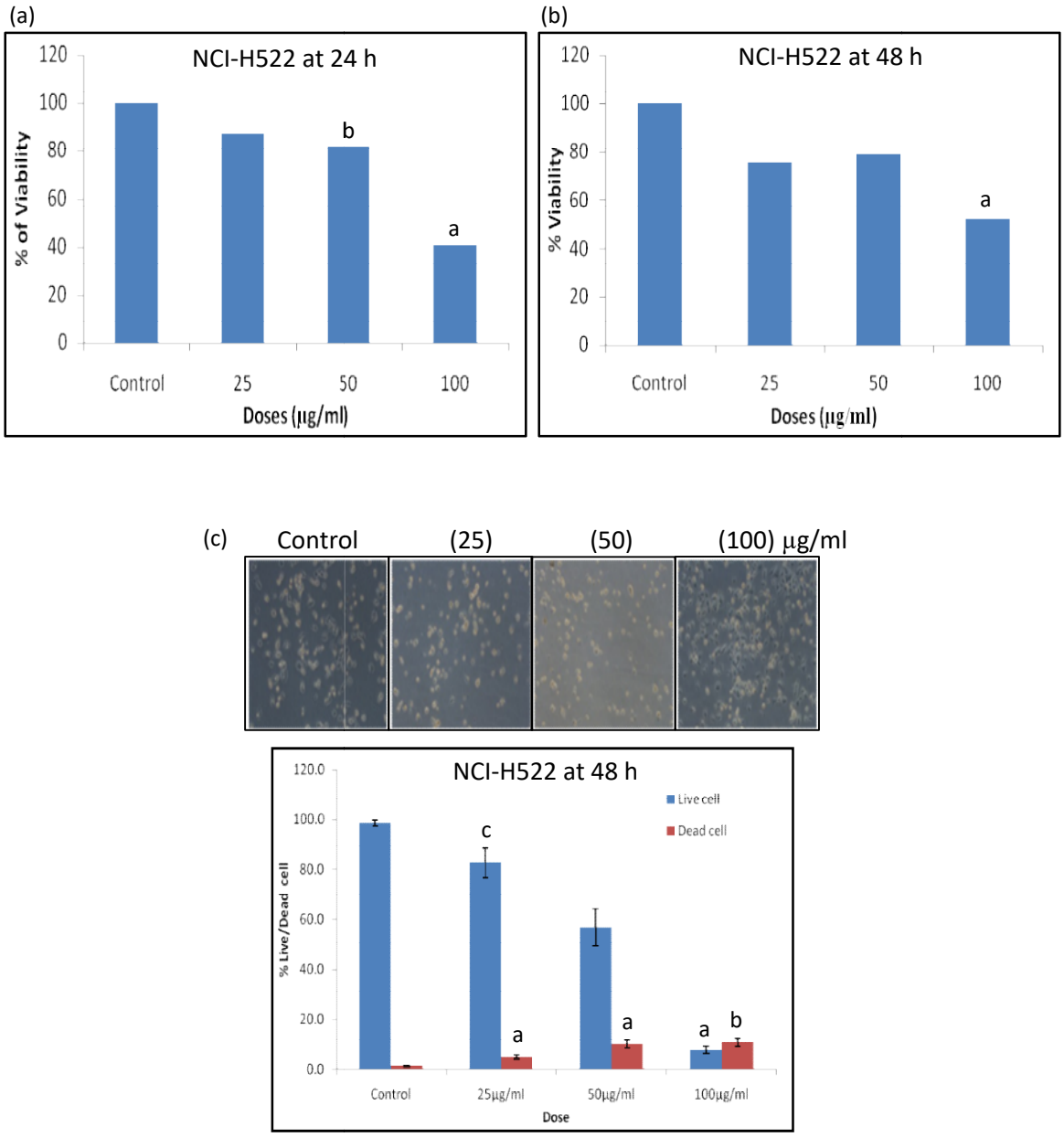

Figure 4.5: Cytotoxic effects of (a) CAN FP at 24 h and (b) CAN FP at 48 h against NCI-H522 cells, measured by MTT based method. (c) Cell counting assay of NCI-H522 cells against CAN FP measured by trypan blue dye exclusion method. The viability is calculated as % of control (100%) Values were expressed as mean ± sem; n=3. Error bars represent standard deviation [a] Significantly different ($p \leq 0.001$) against untreated control. [b] Significantly different ($p \leq 0.01$) against untreated control. [c] Significantly different ($p \leq 0.05$) against untreated control.

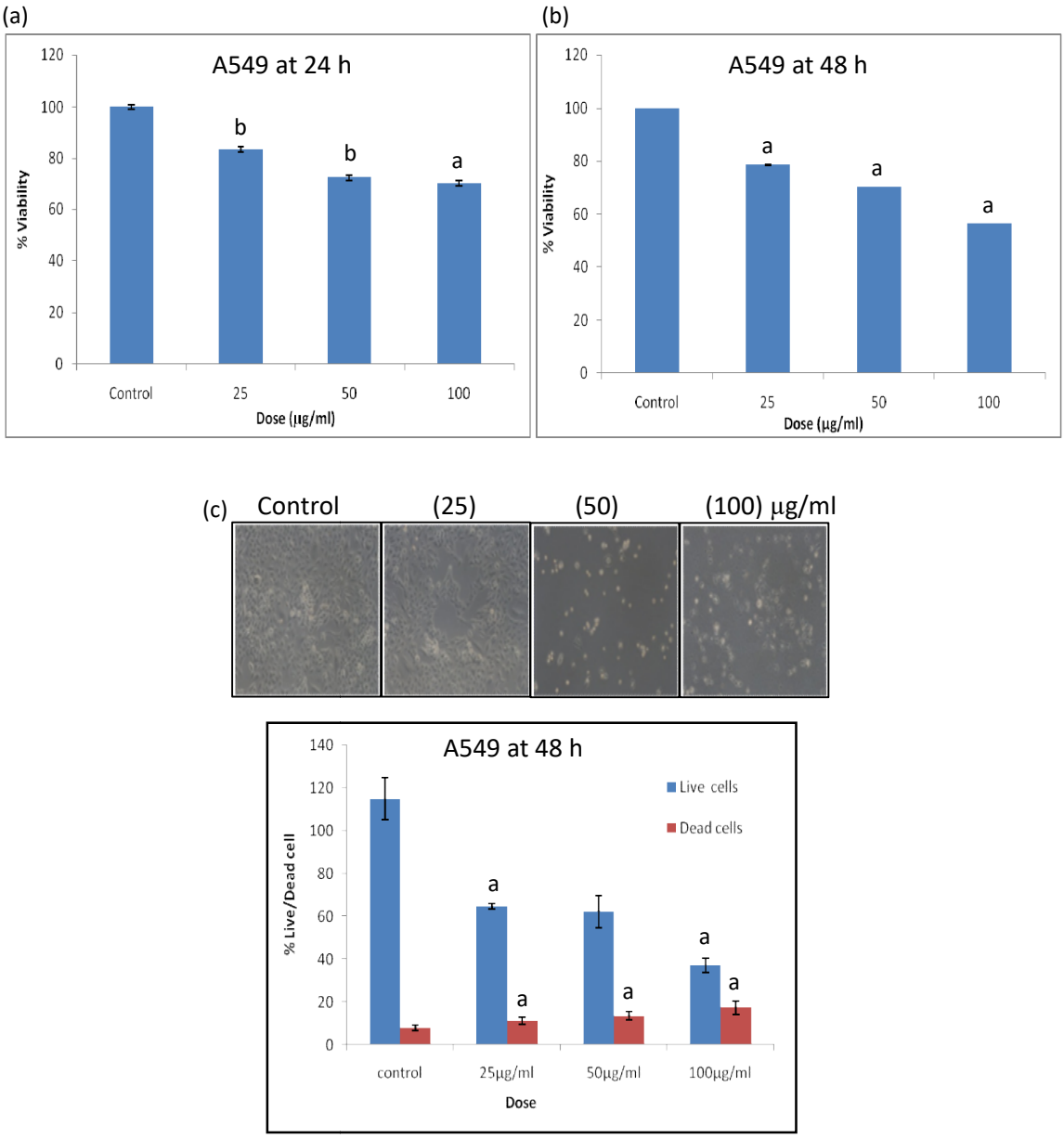

Figure 4.6: Cytotoxic effects of (a) CAN BP at 24 h and (b) CAN BP at 48 h against A549 cells, measured by MTT based method. (c) Cell counting assay of A549 cells against CAN BP measured by trypan blue dye exclusion method. The viability is calculated as % of control (100%) Values were expressed as mean ± sem; n=3. Error bars represent standard deviation [a] Significantly different ($p \leq 0.001$) against untreated control. [b] Significantly different ($p \leq 0.01$) against untreated control.

4.3. CAN free phenolic and CAN bound phenolic induced apoptosis in lung cancer cell lines detection by AO/EtBr double staining and validation by flowcytometry using Annexin V-FITC and PI

AO/EtBr dye staining was performed on lung cancer cells exposed with 25 µg/ml, 50 µg/ml, and 100 µg/ml of phenolic extracts of CAN to identify if the cells undergo necrosis, apoptosis, or a combination of both. Acridine Orange (AO) may readily enter the regular and initial apoptotic cells with intact membranes, and flash green fluorescence upon attaching to DNA, making it possible to detect fundamental morphological variations in apoptotic cells using the double AO/EtBr fluorescence labeling approach. Varying fluorescence is seen at various phases of apoptosis, which serves as an indicator of these processes; for example, green/yellow indicates an intact or early apoptotic cell, whereas orange indicates late apoptotic and red indicates a dead cell. Since AO/EtBr staining may be used to both qualitatively and quantitatively identify apoptosis, it is widely accepted as a reliable approach for doing so.

The degree of induced apoptosis by phenolic extracts of CAN in lung cancer cells was further confirmed by flowcytometry. The treated cells were stained with Annexin V-FITC and Propidium Iodide (PI) after 48 hours of incubation with different concentration of CAN Phenolics. As during apoptosis, loss of plasma membrane integrity leads to externalization of phosphatidylserine which is selectively detected by Annexin V-FITC and on the other hand PI permeates the cell membrane and detects necrotic cells.

The exposure of CAN free and CAN bound phenolics shows induction of apoptosis in A549 cells in dose dependent manner after 48 h of treatment (Figure 4.7, 4.9). The CAN free phenolics also stimulate apoptosis in NCI-H522 cells in dose dependent manner (Figure 4.8). We could also see similar effect in NCI-H23 cells using fluorescence microscope (Figure 4.10). The percentage of late apoptotic and necrotic cells significantly increases in all three cell lines. The results of induced apoptosis detected by fluorescence microscopic is further confirmed by flowcytometry in A549, NCI-H522 cells.

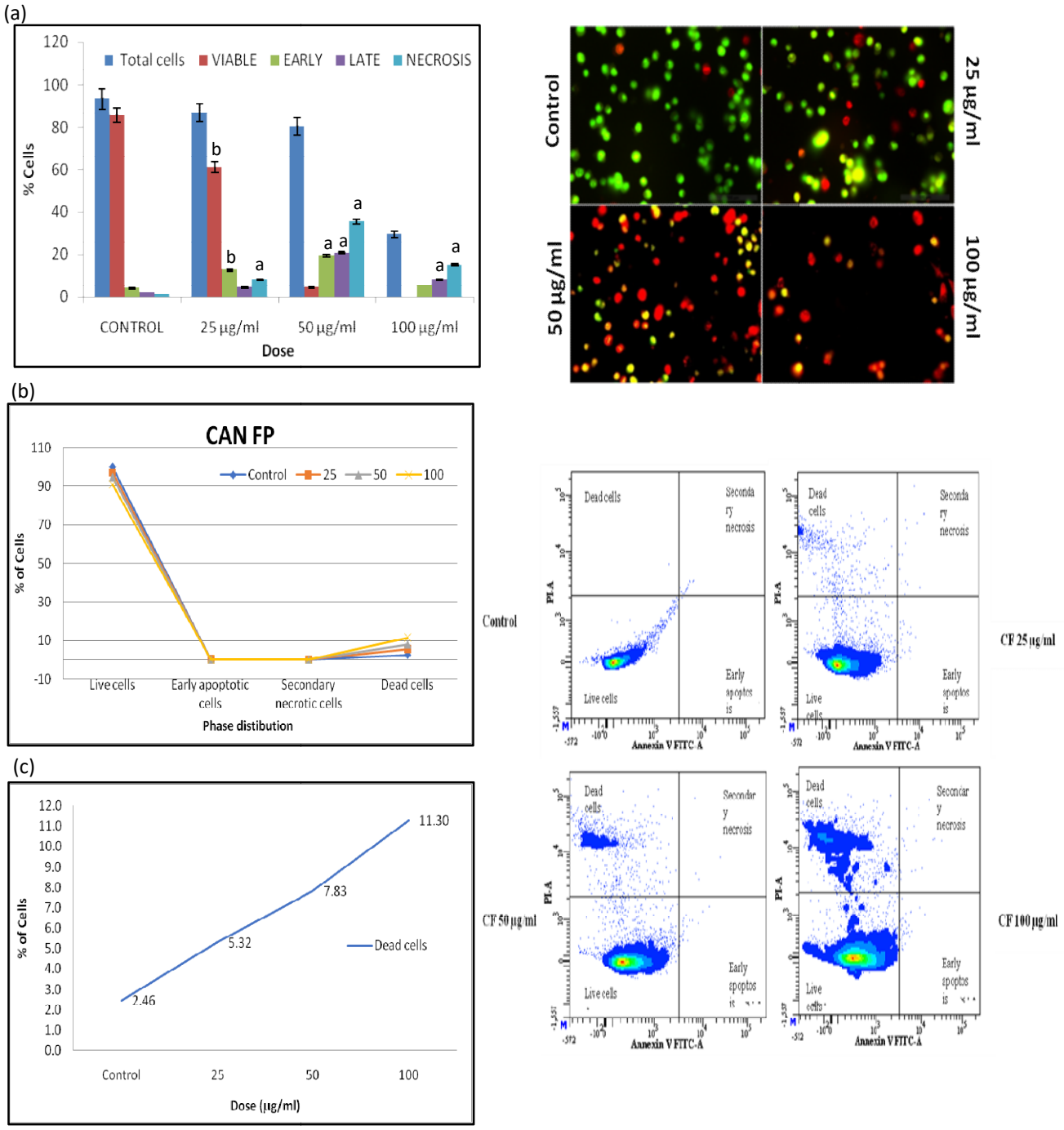

Figure 4.7: AO/EtBr staining of A549 cells treated with (a) CAN free phenolics for 48 h. The cells could be divided into viable, early apoptotic, late apoptotic and necrotic/dead cells. (b), (c) Effect of CAN free phenolics on apoptosis of A549 cell lines after 48 h of treatment. The pictorial representation of pattern of apoptosis phase distribution is shown in contour plot of Annexin V-FITC/PI for evaluation of apoptosis. Values were expressed as mean ± sem; n=3. Error bars represent standard deviation [a] Significantly different ($p \leq 0.001$) against untreated control. [b] Significantly different ($p \leq 0.01$) against untreated control.

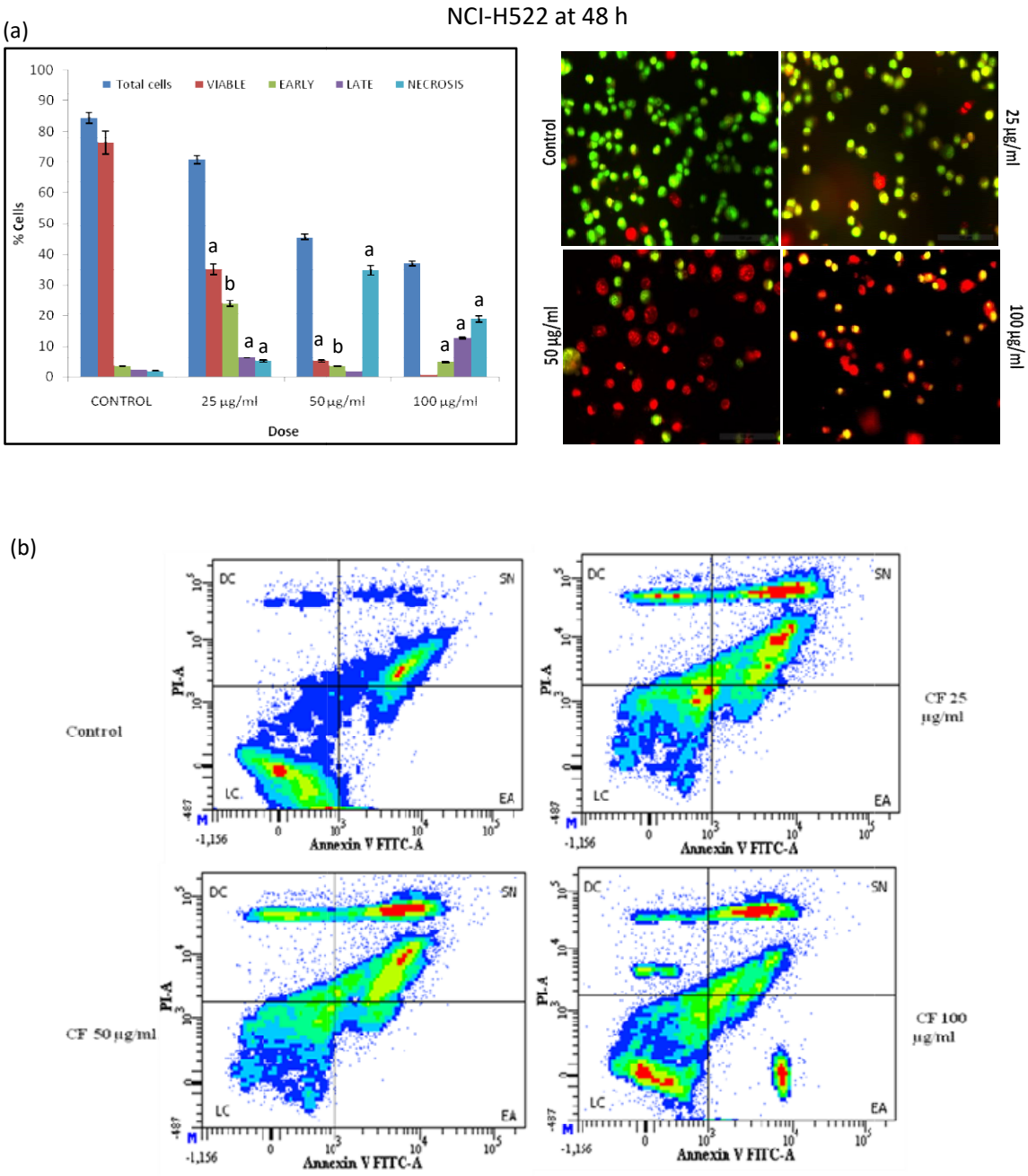

Figure 4.8: AO/EtBr staining of NCI-H522 cells treated with (a) CAN free phenolics for 48 h. The cells could be divided into viable, early apoptotic, late apoptotic and necrotic/dead cells. (b) Effect of CAN free phenolics on apoptosis of NCI-H522 cell lines after 48 h of treatment. The pictorial representation of pattern of apoptosis phase distribution is shown in contour plot of Annexin V-FITC/PI for evaluation of apoptosis. Values were expressed as mean ± sem; n=3. Error bars represent standard deviation [a] Significantly different ($p \leq 0.001$) against untreated control. [b] Significantly different ($p \leq 0.01$) against untreated control.

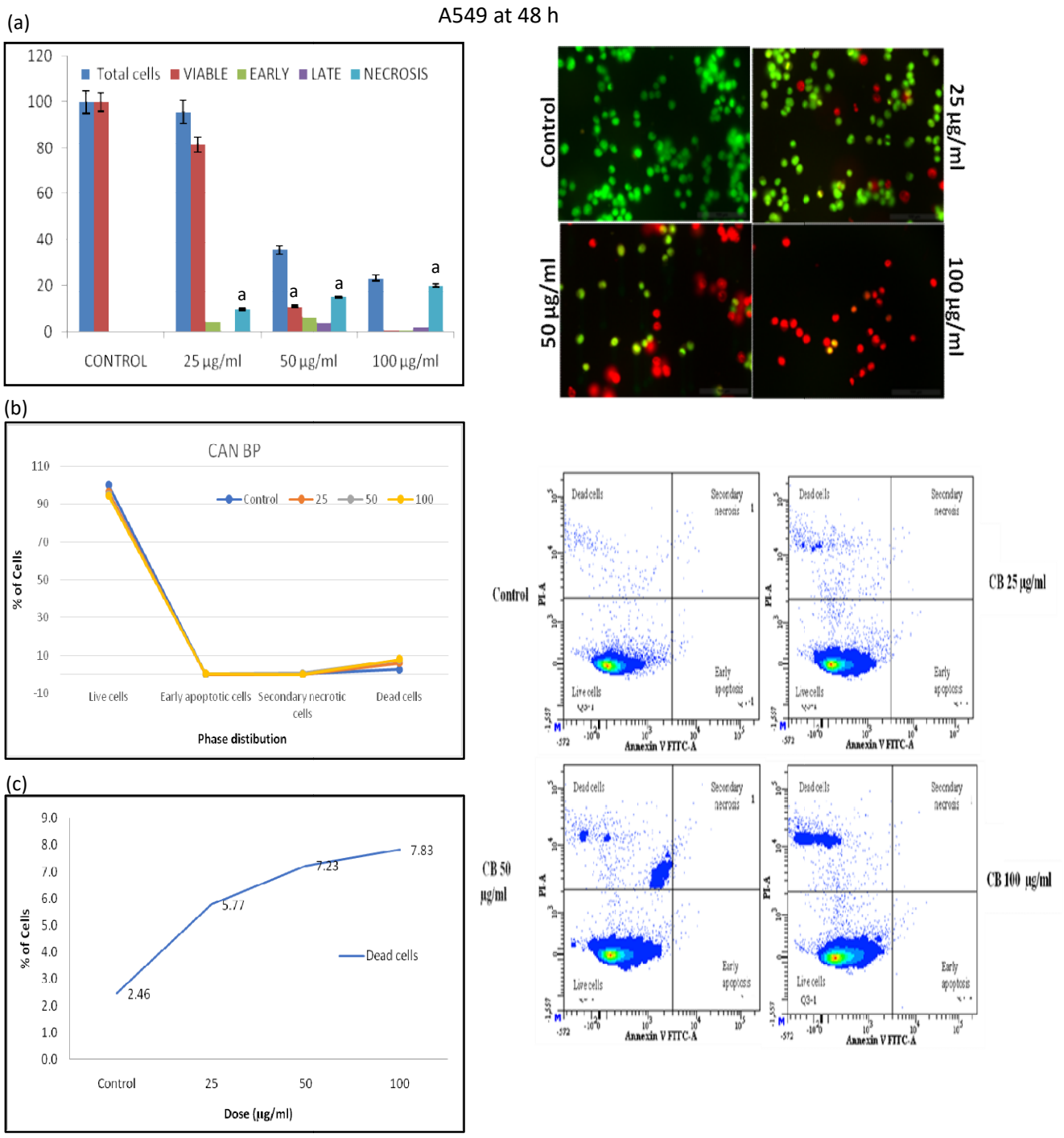

Figure 4.9: AO/EtBr staining of A549 cells treated with (a) CAN bound phenolics for 48 h. The cells could be divided into viable, early apoptotic, late apoptotic and necrotic/dead cells. (b), (c) Effect of CAN bound phenolics on apoptosis of A549 cell lines after 48 h of treatment. The pictorial representation of pattern of apoptosis phase distribution is shown in contour plot of Annexin V-FITC/PI for evaluation of apoptosis. Values were expressed as mean ± sem; n=3. Error bars represent standard deviation [a] Significantly different ($p \leq 0.001$) against untreated control. [b] Significantly different ($p \leq 0.01$) against untreated control.

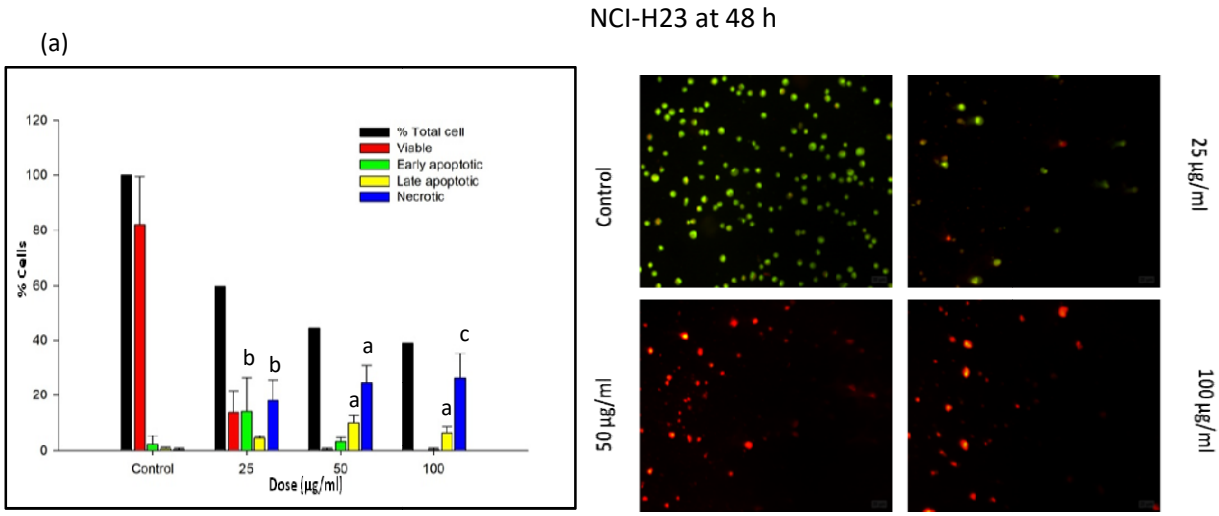

Figure 4.10: AO/EtBr staining of NCI-H23 cells treated with (a) CAN free phenolics for 48 h. The cells could be divided into viable, early apoptotic, late apoptotic and necrotic/dead cells. Values were expressed as mean ± sem; n=3. Error bars represent standard deviation [a] Significantly different ($p \leq 0.001$) against untreated control. [b] Significantly different ($p \leq 0.01$) against untreated control. [c] Significantly different ($p \leq 0.05$) against untreated control.

4.4. CAN free phenolic and CAN bound phenolic induced autophagy and lipid accumulation in lung cancer cell lines detection by fluorescence microscopy, flowcytometry and Oil Red O staining

Autophagy being the second form of cell death in cancer cells by formation of acidic vesicular organelles (AVOs) followed by lysosomal degradation of cellular components. The detection and quantification of autophagosome production in lung cancer cells was done using flow cytometry as well as microscopic examination. The microscopic investigation of A549 cell lines showed that numbers of autophagic vacuoles were significantly decreased in number but size of AVOs increased after 48 hours of exposure to CAN free phenolic fraction (25 µg/ml, 50 µg/ml, 100 µg/ml) compared to control cells (Figure 4.11). In case of NCI-H23 cells we have observed significant increase in numbers of autophagic vacuoles and size of AVOs after 48 hours of exposure to CAN free phenolic fraction (Figure 4.12). We further confirmed the result of induced autophagy by using flowcytometry in A549 cells. We have observed the increase in mean fluorescent intensity in treated cells indicating the percentage of fold change of acid vesicles which validates the above findings (Figure 4.11).

Further we have analyzed the lipid accumulation in response to the CAN phenolic fraction in A549 and NCI-H23 cells using Oil Red O staining (40X). Cells treated with CAN free phenolic (25 µg/ml, 50 µg/ml, 100 µg/ml) for 48 hours exhibits a lipid accumulation phenotype (Figure 4.11, 4.12). The observed significant increase in lipid accumulation in lung cancer cells indicated cellular stress induced by the plant fraction which might correlate to autophagy pathway.

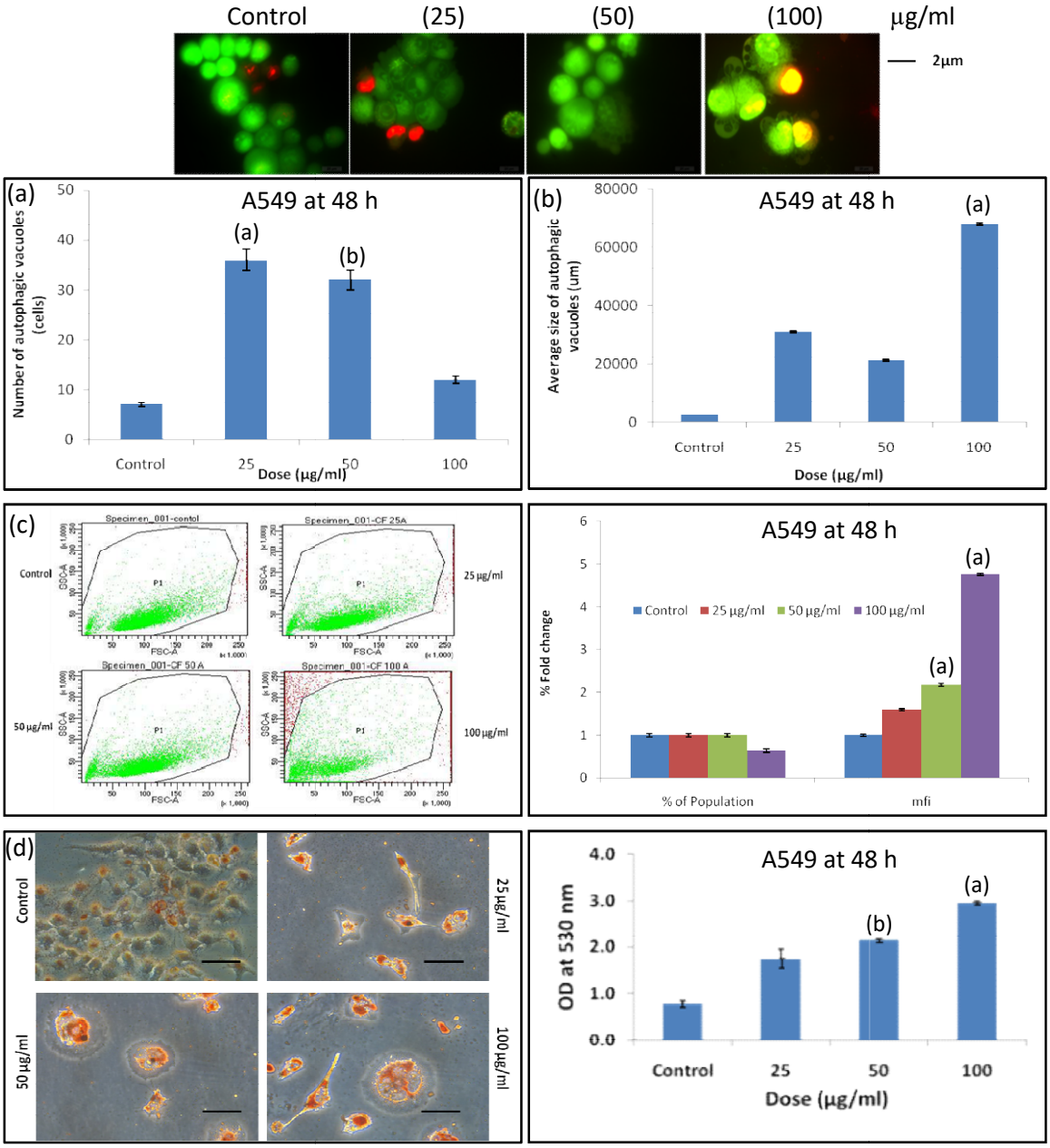

Figure 4.11: Effect of CAN FP on A549 autophagosome formation. (a) Number of autophagosome generation (b) Average size of the autophagosome (c) The data are represented in scattered plot along with bar graph depicting fold changes in vesicle formation. (d) Oil Red O staining of A549 cell lines upon CAN FP treatment for 48 h. Values were expressed as mean ± sem; n=3. Error bars represent standard deviation [a] Significantly different ($p \leq 0.001$) against untreated control. [b] Significantly different ($p \leq 0.01$) against untreated control.

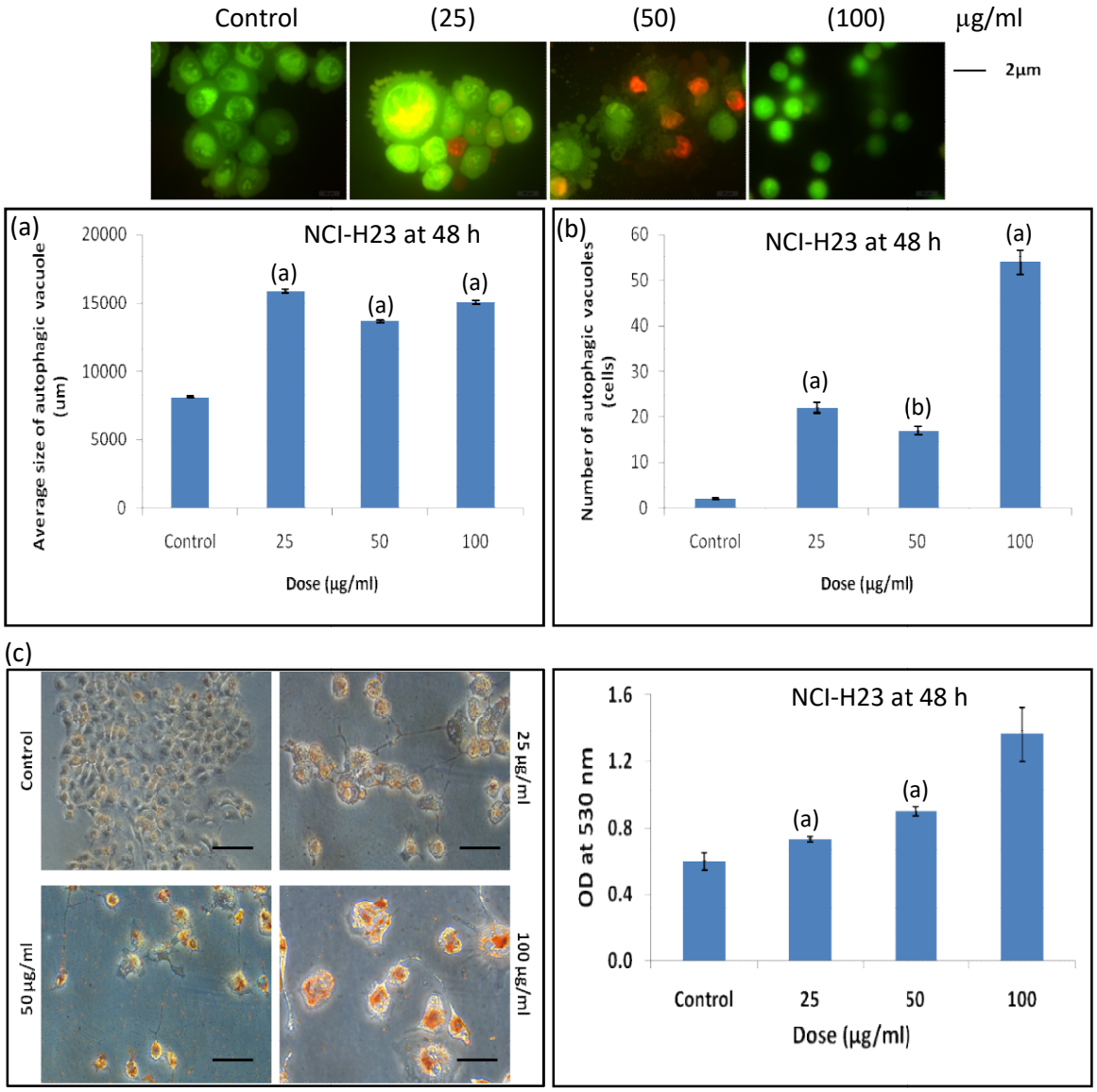

Figure 4.12: Effect of CAN FP on NCI-H23 autophagosome formation. (a) Average size of the autophagosome (b) Number of autophagosome generation (c) Oil Red O staining of NCI-H23 cell lines upon CAN FP treatment for 48 h. Values were expressed as mean ± sem; n=3. Error bars represent standard deviation [a] Significantly different ($p \leq 0.001$) against untreated control. [b] Significantly different ($p \leq 0.01$) against untreated control.

4.5. Effect of CAN free phenolic and CAN bound phenolic in intracellular ROS and MMP generation detected by flow cytometry

In this section, we have used flowcytometry with DCFDA-FITC-A and Rhodamine-123 to evaluate the propensity of CAN free Phenolic and CAN bound phenolic fraction (25 µg/ml, 50 µg/ml, 100 µg/ml) to produce intracellular ROS and MMP in the exposed lung cancer cell lines. The degree of fluorescence by oxidized DCF is measured after CAN phenolics treatment. Diminished fluorescence in the presence of Rhodamine-123, a fluorescent dye used to evaluate mitochondrial membrane integrity or mitochondrial membrane depolarization, represented the loss of the MMP.

We have observed a significant increase in intracellular ROS level in A549 cells as the mean fluorescence intensity increases after 48 hours of CAN free phenolic fraction exposure. The result demonstrates that the treated A549 cell shows an increase in number of ROS-positive cells relative to untreated cells by 2.8 ($p \leq 0.001$) folds. Also the MMP activity was significantly increased in dose dependent manner by 1.18-1.56 ($p \leq 0.001$) folds compared to control (Figure 4.13). On the other hand in A549 cells, the ROS level increased by 0.86 ($p \leq 0.001$) folds and MMP fold change rises from 0.9 to 1.0 ($p \leq 0.001$) when treated with CAN Bound Phenolic fraction for 48 hours (Figure 4.14).

Hence the CAN free and CAN bound phenolics treated cancer cells exhibit increase in intracellular ROS levels indicated by increase in mean fluorescent intensity thus resulted in mitochondrial dysfunction. The finding is supported by decrease in mitochondrial membrane potential and/or hyper polarization with increase in dose of the extract. This indicates that the phenolics treated cells undergo cellular stress and overall cell death in cancer cells either by apoptosis or autophagy,

(a)

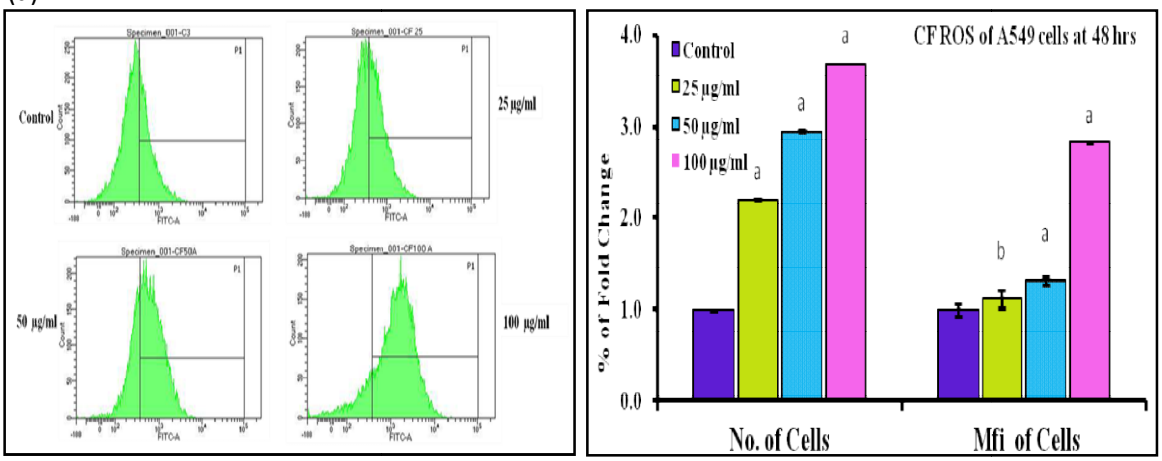

(b)

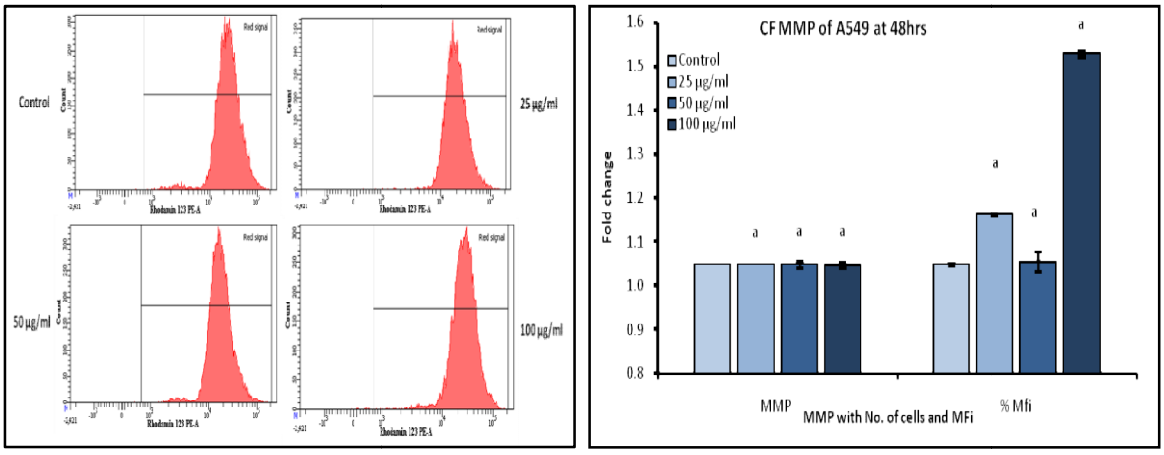

Figure 4.13: Effect of CAN free phenolics on (a) intracellular ROS level of A549 cells upon treatment for 48 h. The histogram and corresponding bar graph represents the fold change in ROS generation after 48 h of plant fraction treatment. (b) Mitochondrial membrane potential of A549 cells. The histogram and corresponding bar graph represents the fold change in MMP after 48 h of plant fraction treatment. Values were expressed as mean ± sem; n=3. Error bars represent standard deviation [a] Significantly different ($p \leq 0.001$) against untreated control. [b] Significantly different ($p \leq 0.01$) against untreated control.

(a)

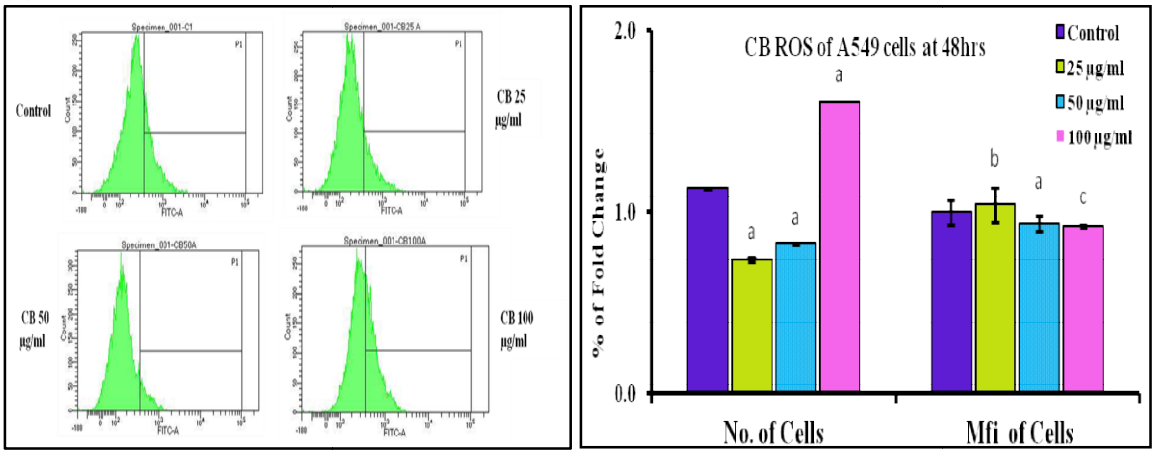

(b)

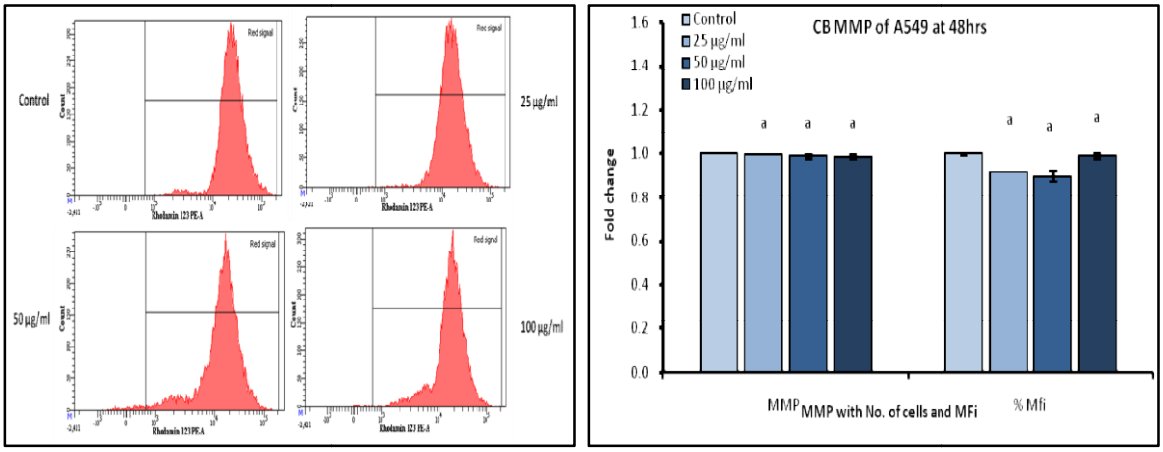

Figure 4.14: Effect of CAN bound phenolics on (a) intracellular ROS level of A549 cells upon treatment for 48 h. The histogram and corresponding bar graph represents the fold change in ROS generation after 48 h of plant fraction treatment. (b) Mitochondrial membrane potential of A549 cells. The histogram and corresponding bar graph represents the fold change in MMP after 48 h of plant fraction treatment. Values were expressed as mean ± sem; n=3. Error bars represent standard deviation [a] Significantly different ($p \leq 0.001$) against untreated control. [b] Significantly different ($p \leq 0.01$) against untreated control. [c] Significantly different ($p \leq 0.05$) against untreated control.

4.6. Cell cycle analysis in lung cancer cell lines using CAN free phenolic and CAN bound phenolics

As most of the known anticancer drugs act by altering cell cycle distribution of cancer cells at G0/G1, S, G2/M phase and leading to cell death or apoptosis. We have investigated the effect of CAN free and CAN bound phenolic fractions (25 µg/ml, 50 µg/ml, 100 µg/ml) in cell cycle phase distribution in lung cancer cell lines by quantifying the DNA content using Propidium Iodide (PI) fluorescence in flowcytometer.

We have observed a significant increase in A549 cell population at S and G2/M phase after 48 hours when exposed to CAN free phenolics (Figure 4.15). The population of the treated cells was arrested in S phase 41.55-74.40% ($p \leq 0.001$) and in G2/M phases 11.35-31.45% ($p \leq 0.001$) with respect to the control cells 14.35% and 8.55% respectively. A considerable increase in the S-Phase and G2/M cell population was observed after 48 hours of treatment with CAN free phenolic in NCI-H522 cells. The distribution of NCI-H522 cells were at S phase 38.30% ($p \leq 0.001$) and at G2/M phase 20.50% ($p \leq 0.001$). The cell population in both A549 and NCI-H522 cell lines undergoes apoptosis by 5.2-6.8% ($p \leq 0.001$).

The A549 cells exposed to 25 µg/ml, 50 µg/ml, and 100 µg/ml of CAN bound phenolic extract showed a considerable increase in cell population and arrest at the G0/G1 phase by 79.45% ($p \leq 0.01$) in 48 hours (Figure 4.16). We have observed similar pattern of cell cycle arrest in A549 cell lines when treated with Cisplatin drug (0-2.5mM/ml). The A549 cell populations were arrested in S phase 22.20-45.10% ($p \leq 0.001$) and at G2/M phase 12.4-46.68% ($p \leq 0.001$) with respect to the control 12.65% and 11.15% respectively (Figure 4.16). Similar to the CAN free phenolics action in A549 cells the Cisplatin treated cells undergoes apoptosis by 5.9% ($p \leq 0.001$) when treated with 0-2.5mM/ml concentration after 48 hours.

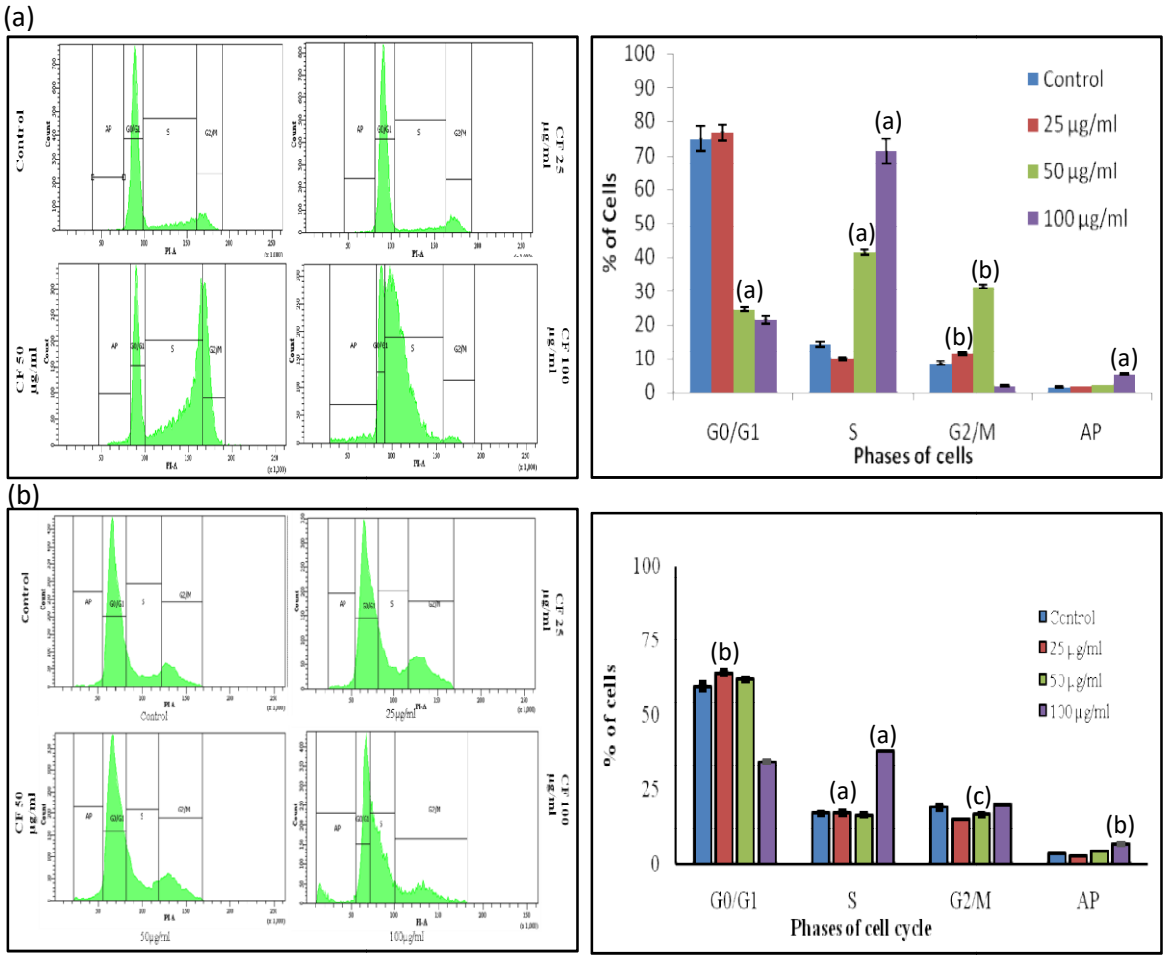

Figure 4.15: Effect of CAN free phenolics on cell cycle distribution of (a) A549 cells and (b) NCI-H522 cells after 48 h of incubation. Histogram display of DNA content (x-axis, PI-fluorescence) vs. cell count (y-axis) and bar graph representation of cell cycle distribution at G0/G1, S and G2/M phase. Values were expressed as mean ± sem; n=3. Error bars represent standard deviation [a] Significantly different ($p \leq 0.001$) against untreated control. [b] Significantly different ($p \leq 0.01$) against untreated control. [c] Significantly different ($p \leq 0.05$) against untreated control.

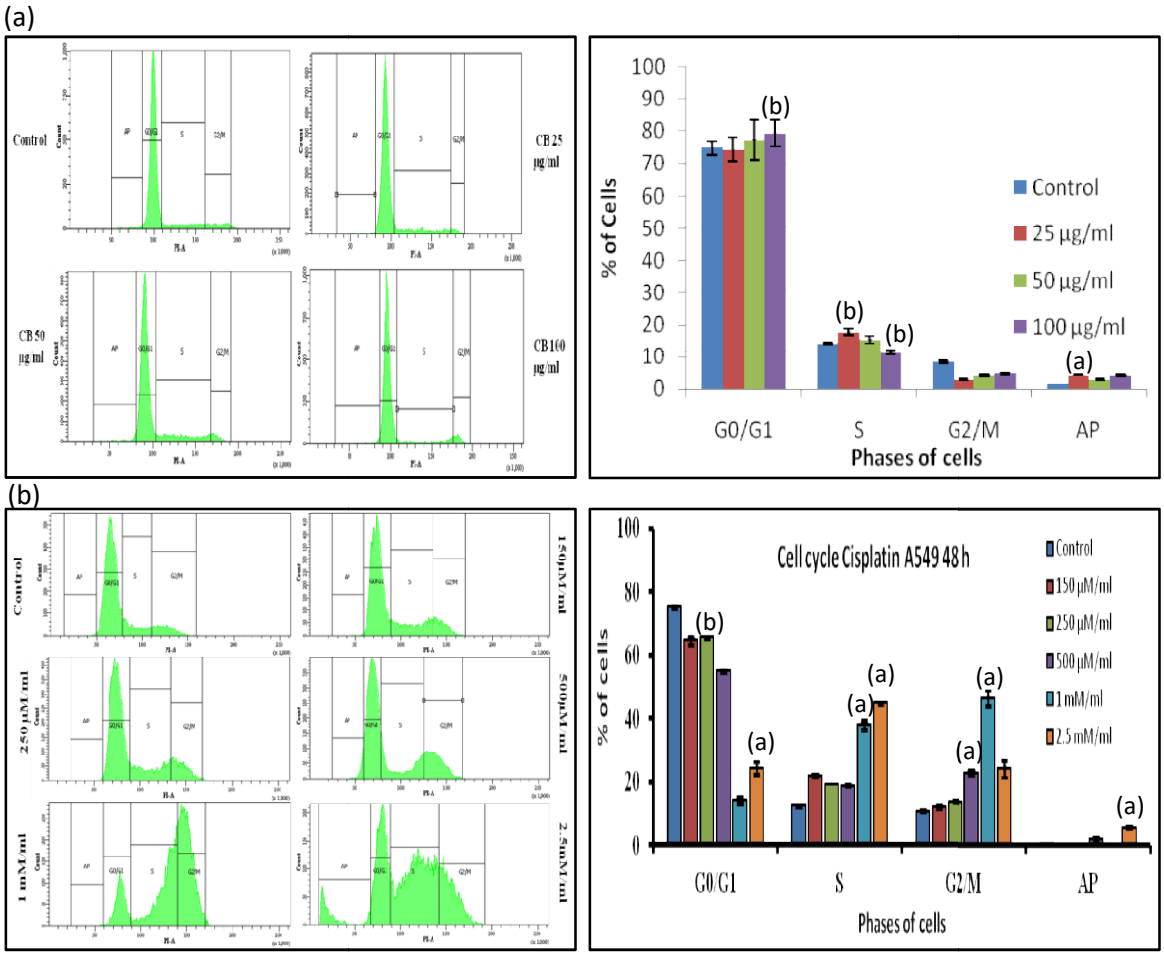

Figure 4.16: Effect of (a) CAN bound phenolics on cell cycle distribution of A549 cells and (b) Cisplatin on cell cycle distribution of A459 cells after 48 h of incubation. Histogram display of DNA content (x-axis, PI-fluorescence) vs. cell count (y-axis) and bar graph representation of cell cycle distribution at G0/G1, S and G2/M phase. Values were expressed as mean ± sem; n=3. Error bars represent standard deviation [a] Significantly different ($p \leq 0.001$) against untreated control. [b] Significantly different ($p \leq 0.01$) against untreated control.

4.7. Effect of CAN free phenolic and CAN bound phenolic in cell proliferation of lung cancer cell lines using CFSE labeled flowcytometry

The effect of CAN free and CAN bound phenolics in overall lung cancer cell proliferation was monitored using intracellular dye, carboxylfluorescein succininmidyl ester (CFSE) in flowcytometry. As with each cell division, the fluorescent dye distributes throughout the daughter cells causing a drop in fluorescence intensity in proliferating cells is therefore measured by flowcytometry.

The exposure of A549 cells with CAN free phenolic fractions for 72 hours shows significant reduction in cell proliferation up to 5.48% (($p \leq 0.001$) with increase in dose of the extract (25 µg/ml, 50 µg/ml, 100 µg/ml). In case of NCI-H522 cell lines the proliferation rate is inhibited up to 71.54% ($p \leq 0.001$) (Figure 4.17). Although no significant change in rate of proliferation was observed in case of CAN bound phenolics treatment in A549 cells. Interestingly the proliferation rate of human PBMCs was increased in dose dependent manner upon exposure to either phenolic fractions of CAN (Figure 4.18). This observation corresponds to the cell viability of CAN phenolic fractions measured by MTT based method (Figure 4.2). Thus from the present findings we can conclude that the plant phenolic fractions inhibiting overall cell proliferation in lung cancer cell lines in dose dependent manner and on the other hand enhances cell proliferation in human PBMCs.

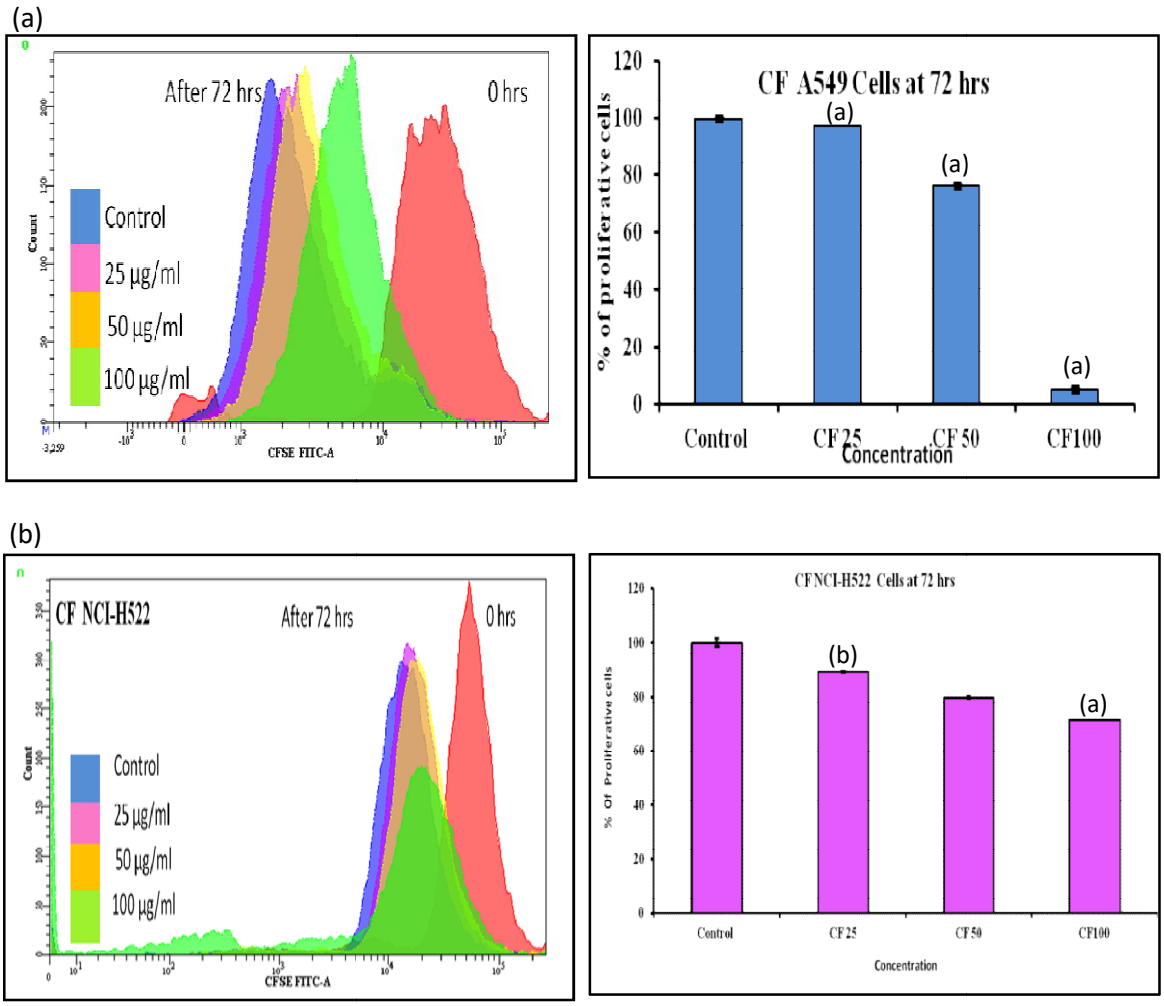

Figure 4.17: Effect of CAN free phenolics on cell proliferation of CFSE labelled lung cancer cell lines incubated for 72 h; (a) CAN free phenolics in A549 cells (b) CAN free phenolics in NCI-H522 cells. The CFSE labelled cells at 0 h were negative control. The reduction of CFSE fluorescence was measured by flow cytometry at 72 h. Values were expressed as mean ± sem; n=3. Error bars represent standard deviation [a] Significantly different ($p \leq 0.001$) against untreated control. [b] Significantly different ($p \leq 0.01$) against untreated control.

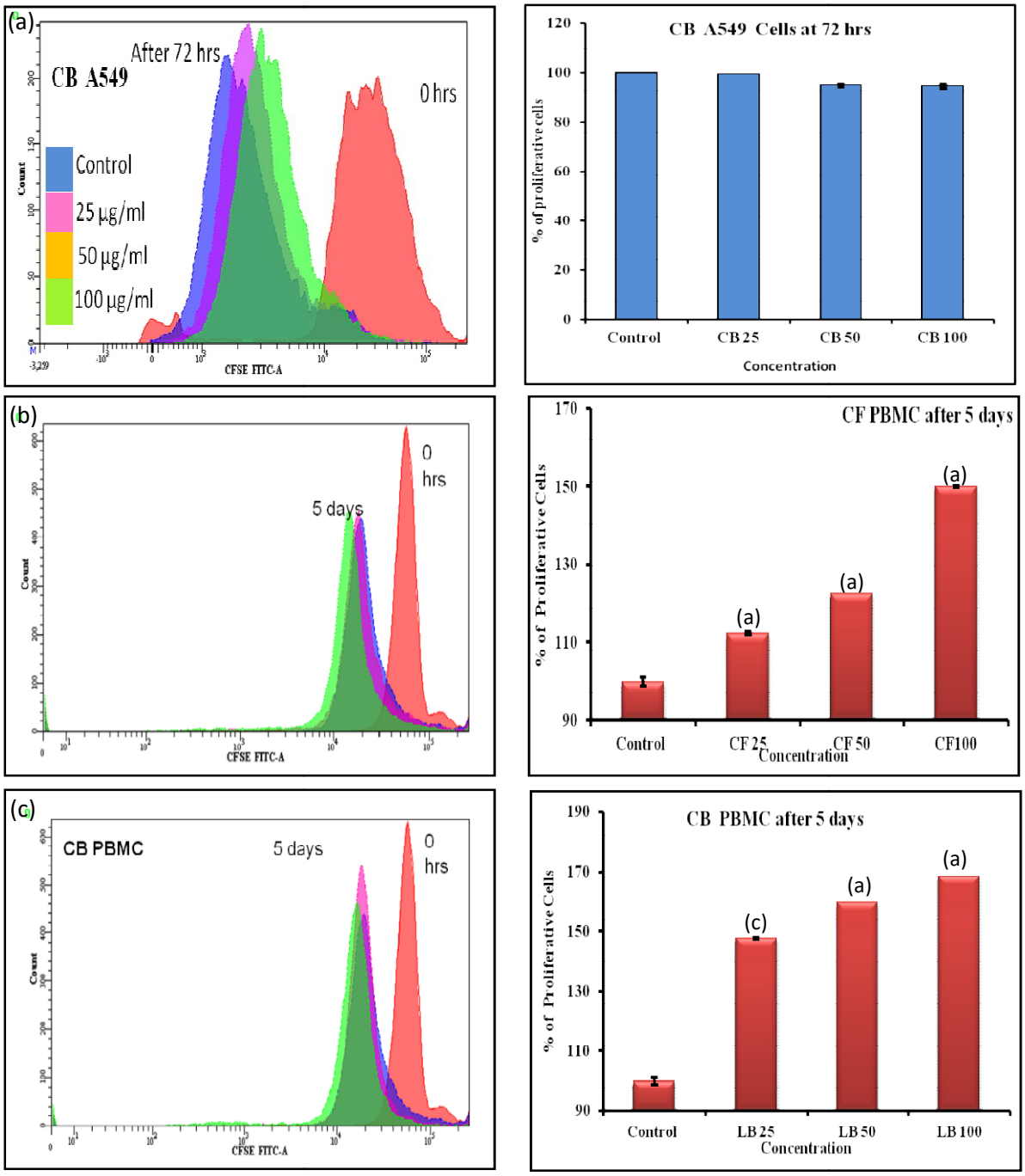

Figure 4.18: Effect of CAN bound phenolics on cell proliferation of CFSE labelled (a) A549 cells incubated for 72 h; (b) CAN free phenolics in human PBMCs for 5 days (c) CAN bound phenolics in human PBMCs for 5 days. The CFSE labelled cells at 0 h were negative control. The reduction of CFSE fluorescence was measured by flow cytometry at 72 h and 120 h. Values were expressed as mean ± sem; n=3. Error bars represent standard deviation [a] Significantly different ($p \leq 0.001$) against untreated control. [c] Significantly different ($p \leq 0.05$) against untreated control.

4.8. The effect of CAN free phenolic and CAN bound phenolic fractions in clonogenic and cell migration ability in lung cancer cell lines

Cell migration and colony formation is an essential cellular behavior of cancer cells that plays a crucial role in disease aggressiveness and metastasis. Therefore, reducing this clonogenic and migratory potential of cancer cells is essential for both successful lung cancer eradication and disease prevention. This motivated to study the inhibitory effect CAN free phenolic and CAN bound phenolic fractions in colony formation and cell migration in lung cancer cell lines.

The lung cancer cells A549 and NCI-H23, the clonogenicity was significantly inhibited in dose dependent manner as well as the rate of migration was subdued remarkably in increase in dose (25 µg/ml, 50 µg/ml, 100 µg/ml) when exposed to CAN free phenolics for 48 hours (Figure 4.19). The clonogenicity of A549 cells were remarkably reduced to 10% and migratory efficacy is inhibited up to 8% when treated CAN free phenolics. Likewise, in NCI-H23 cells, the clonogenicity is reduced to less than 5% and the rate of migration is significantly inhibited when treated CAN free phenolics. The data suggest that CAN free phenolics have significantly reduced cell migration without the confounding influence of cell proliferation. The CAN free and CAN bound phenolics also reduced the clonogenicity of NCI-H522 cells to 5% and 30% in done dependent manner (Figure 4.20).

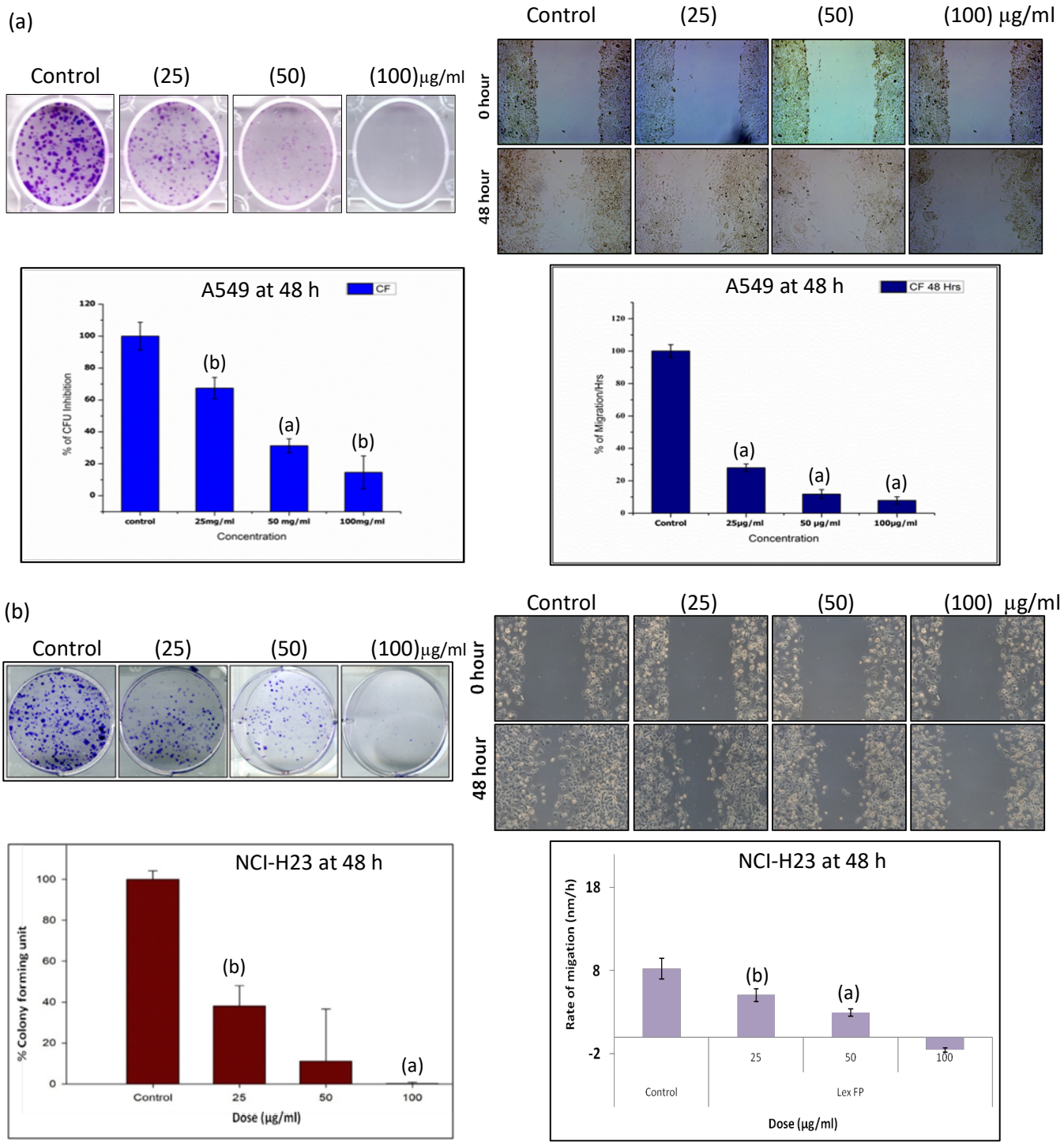

Figure 4.19: Effect of CAN free phenolics on (a) Clonogenic assay and cell migration in A549 cell lines; (b) Clonogenic assay and cell migration in NCI-H23 cell lines. Values were expressed as mean ± sem; n=3. Error bars represent standard deviation [a] Significantly different ($p \leq 0.001$) against untreated control. [b] Significantly different ($p \leq 0.01$) against untreated control.

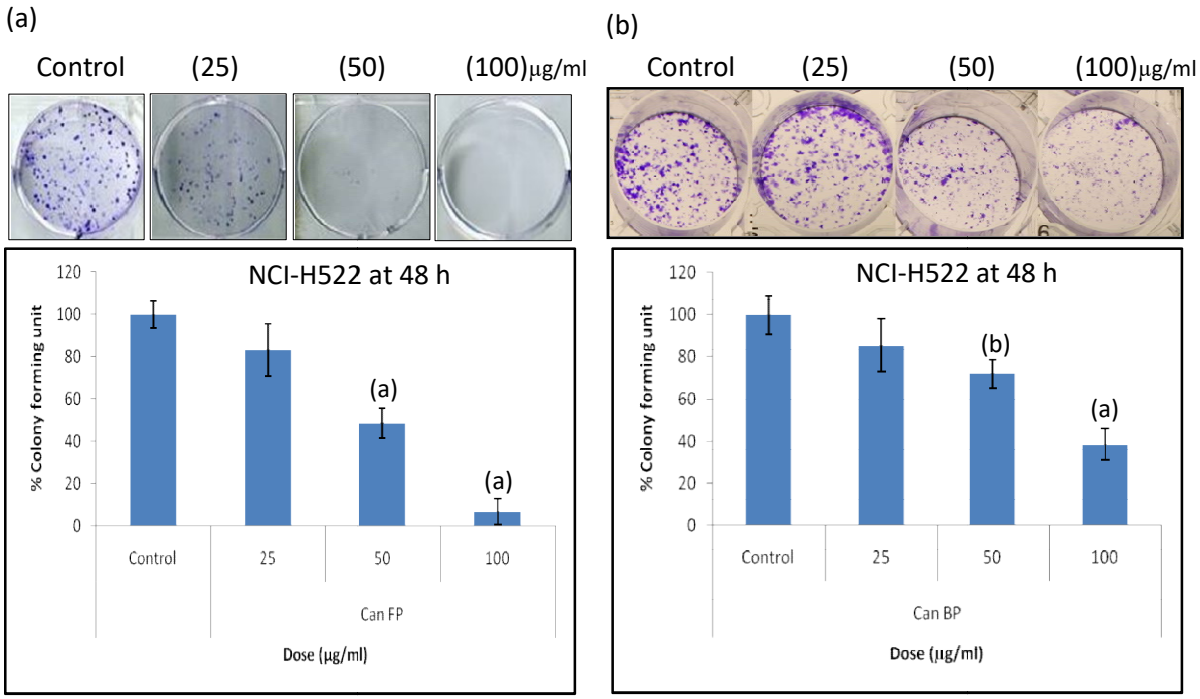

Figure 4.20: Effect of CAN free phenolics on (a) Clonogenic assay in NCI-H522 cell lines; (b) effect of CAN bound phenolics on Clonogenic assay in NCI-H522 cell lines. Values were expressed as mean ± sem; n=3. Error bars represent standard deviation [a] Significantly different ($p \leq 0.001$) against untreated control. [b] Significantly different ($p \leq 0.01$) against untreated control.

4.9. OHRLCMS chromatogram results for CAN free phenolic compound

The major compounds in Lex free phenolic fraction include Genistein, Trolox, Resperpine, Xylitol, 2-Hydroxy-1,4-naphthoquinone, 3,4-Dimethylbenzoic acid, Resorcinol, 6-Gingerol, etc. along with a composite mixture of known anticancer phytochemicals along with some unknown molecular peaks present in the fraction that may have acted over anticancer efficacy (Table 4.1).

OHRLCMS chromatogram of methanolic extract of CAN free phenolic compound are shown in Figure 4.21.

Table 4.1: Anticancer activity of bioactive compounds found in CAN polyphenols.

Compound	Plant source	Inhibition of Cancer
Genisteine	*Flemingia vestita* Benth	Prostrate, Cervix, Colon
Trolox	*Rutaceae* family	Breast, Ovary, Colon
Resperpine	*Rauwolfia vomitoria*	Lung, Ovary, Breast
Xylitol	*Betulaceae* family	Lung, Oral, Pancreas,
2-Hydroxy-1,4-naphthoquinone	*Lawsonia inermis*	Lung, Abdomen, Breast
3,4-Dimethylbenzoic acid	*Viburnum cylindricum*	Lung, Cervical
Resorcinol	*Myristica fatua* Houtt	Lung, Liver, Pancreas
6-Gingerol	*Zingiberaceae* family	Lung, Leukaemia, Breast

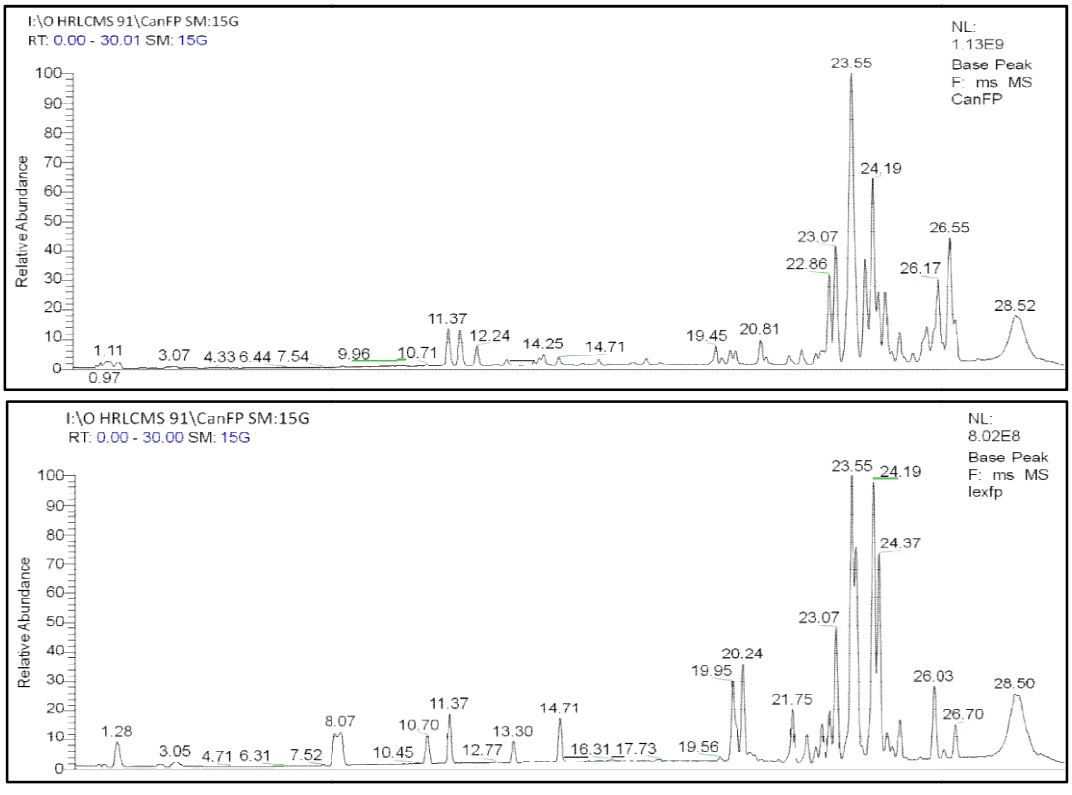

Figure 4.21: OHRLCMS chromatogram of methanolic extract of CAN free phenolic compound

4.10. Animal toxicity of CAN free phenolics in Balb/C mice.

The treatment of CAN free phenolics to Balb/C mice did not cause any toxicity and mortality. The plant phenolics did not alter the test results of hepatotoxicity, nephtotoxicity and hematological parameters as shown in Table 4.2, Table 4.3 and Table 4.4.

Table 4.2: Result of hepatological parameters in Balb/C mice

	Total Protein (g/dL)	Albumin (g/dL)	AST (U/L)	ALT (U/L)	ALKP (U/L)	Total Bilirubin (mg/dL)	Unconj. Bilirubin (mg/dL)	Direct Bilirubin (mg/dL)	Glucose (mg/dL)
Control	**5.67 ± 0.19**	**2.88 ± 0.11**	**129.50 ± 40.19**	**32.50 ± 10.29**	**133.17 ± 21.12**	**0.85 ± 0.24**	**0.05 ± 0.04**	**0.81 ± 0.20**	**125.00 ± 9.57**
Can F P (100 mg/kg body. wt)	**6.69 ± 0.42**	**3.53 ± 0.29**	**144.00 ± 53.25**	**32.60 ± 10.01**	**141.40 ± 40.14**	**1.52 ± 0.56**	**0.00 ± 0.00**	**1.52 ± 0.56**	**110.20 ± 24.89**

Table 4.3: Result of nephrotoxicity parameters in Balb/C mice

	BUN (mg/dL)	Creatinin (mg/dL)	Sodium (mmol/L)	Potassium (mmol/L)
Control	**14.92 ± 3.57**	**0.10 ± 0.02**	**157.17 ± 1.47**	**6.82 ± 0.63**
Can FP (100 mg/kg body. wt)	**19.02 ± 4.53**	**0.12 ± 0.02**	**161.80 ± 3.11**	**8.24 ± 1.01**

Table 4.4: Result of hematological parameters in Balb/C mice

Parameters (Unit)	Control	Can FP
WBC(m/mm^3)	5.85±1.65	5.82±1.50
Lymphocytes (%)	82.42±3.74	80.67±3.01
Monocytes (%)	2.53±0.16	2.4±0.64
Neutrophils (%)	10.68±2.94	12.78±2.14
Eosinophils (%)	3.5±1.38	3.17±1.96
Basophils (%)	0.3±0.09	0.32±0.16
Total RBC(m/mm^3)	9.02±0.30	9.12±0.35
MCV (fl)	49.13±1.21	49.42±1.73
HCt(%)	44.32±1.87	45.05±2.04
MCH (pg)	15.38±0.33	15.93±0.38
MCHC(g/dl)	31.3±0.39	32.2±0.90
RDW	12.78±0.44	12.45±0.29
Hb(g/dl)	13.87±0.52	14.5±0.35

4.11. Effect of CAN free phenolics against A549 induced cancer in athymic nude mice.

In the present study we have done a pilot study in athymic nude mice to understand the antitumor activity of CAN free phenolics against A549 induced carcinoma. The findings suggests that the tumour burden in phenolics treated groups was 94% while the tumourigenicity was inhibited up to 6% with respect to the control. Survival/mortality rate is to be kept in mind before doing the experiments for significance of the results (Figure 4.22).

(a)

(b)

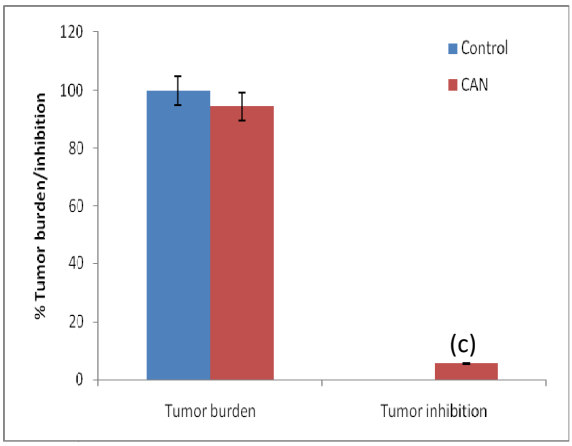

Figure 4.22: Effect of CAN free phenolics on (a) athymic nude mice against A549 induced carcinoma. (b) Bar graph represents the % tumour burden and inhibition. Values were expressed as mean ± sem; Error bars represent standard deviation. [c] Significantly different ($p \leq 0.05$) against untreated control.

Part B- Evaluation of anti-proliferative and pro-apoptotic efficacy of phenolic fraction of *Smilax ovalifolia.*

In this section we are presenting our findings on efficacy of free phenolics and bound phenolics extracted from *Smilax ovalifolia* (LEX). The data generated using standard methods that are commonly used in such studies using *in vitro* and *in vivo* models.

4.12. Cytotoxicity Assay against Human RBCs and PBMCs

To check the toxicity of the selected plant extract we have used the membrane stability activity on human RBCs against Triton-X 100 induced haemolysis and viability of human PBMCs using MTT based method.

As shown in (Figure 4.23) the phenolic extract shows protective role against Triton-X 100 induced haemolysis with respect to the +ve and –ve control. The activity of the plant extract was compared with ascorbic acid. On the other hand, the cell viability was observed at 24 h when the human PBMCs were exposed to either the free phenolic or bound phenolic extract. Cell viability was shown to be higher than the control with rising concentration across all time periods of exposure as shown in (Figure 4.24), suggesting that extract is not toxic to human RBCs and substantially stimulates proliferation in human PBMCs ($p \leq 0.001$).

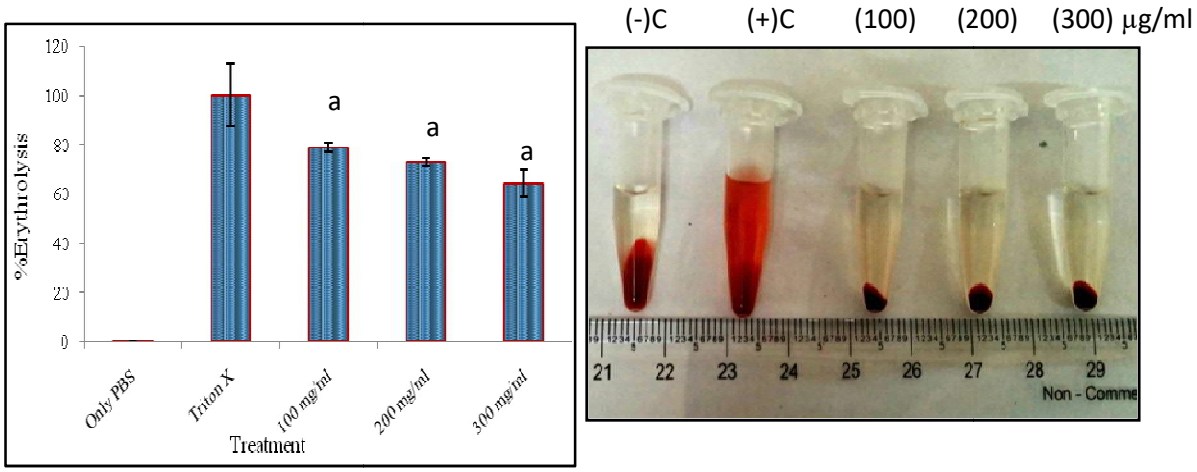

Figure 4.23: Effect of different concentration of LEX on % inhibition of Triton-X induced haemolysis of human erythrocytes incubated in PBS. Values were expressed as mean ± sem; n=3. Error bars represent standard deviation [a] Significantly different ($p \leq 0.001$) against untreated control.

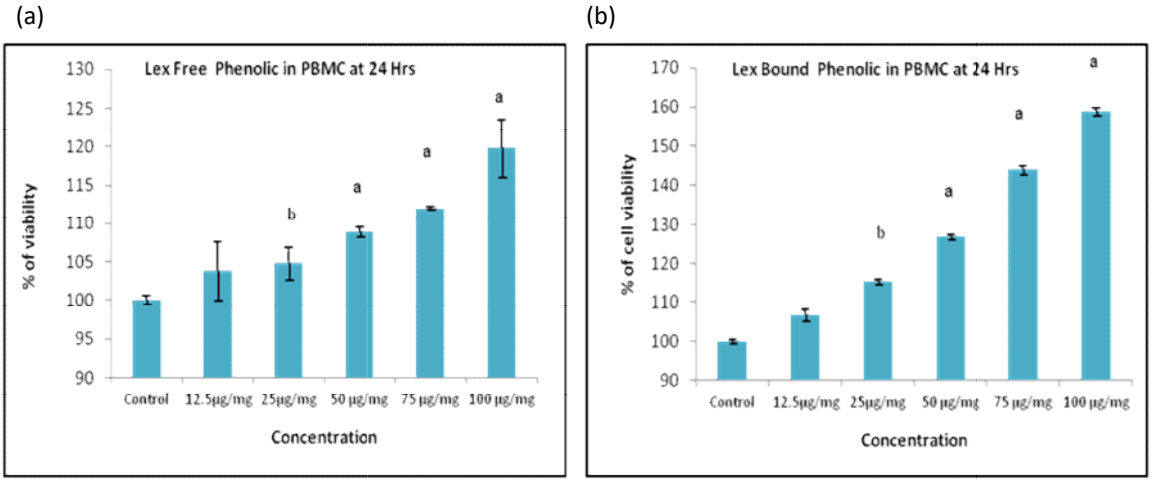

Figure 4.24: Cytotoxic effects of (a) LEX FP at 24 h and (b) LEX BP at 24 h, measured by MTT based method. Values were expressed as mean ± sem; n=3. Error bars represent standard deviation [a] Significantly different ($p \leq 0.001$) against untreated control. [b] Significantly different ($p \leq 0.01$) against untreated control.

4.13. Cytotoxicity effect of LEX free phenolic and LEX bound phenolic on human lung cancer cell lines

LEX free phenolic and LEX bound phenolic extracts were tested for their cytotoxicity on human lung cancer cell lines; A549, NCI-H522 and NCI-H23, using the MTT based method and trypan blue exclusion assay.

The LEX free phenolic and LEX bound phenolic fraction shows inhibition of cell viability on human lung cancer cells at dose dependent manner after 24 and 48 hours of treatment. It also strongly inhibits the overall cell growth in a dose dependent manner in all three cell lines with noticeably reduced in IC50 values (Figure 4.25, 4.26, 4.27 and 4.28). The number of death cell substantially increases with respect to the dose and time of incubation.

The plant fractions shows selective cytotoxicity in cancer cells yet remain non toxic to normal human cells, suggesting the presence of specific photochemical that significantly targets cancer cells.

Exploration of such plant based active compound would enlighten the discovery of new anticancer therapeutics and reduce the cost and other limitations that tagged with conventional anticancer approach/module present today.

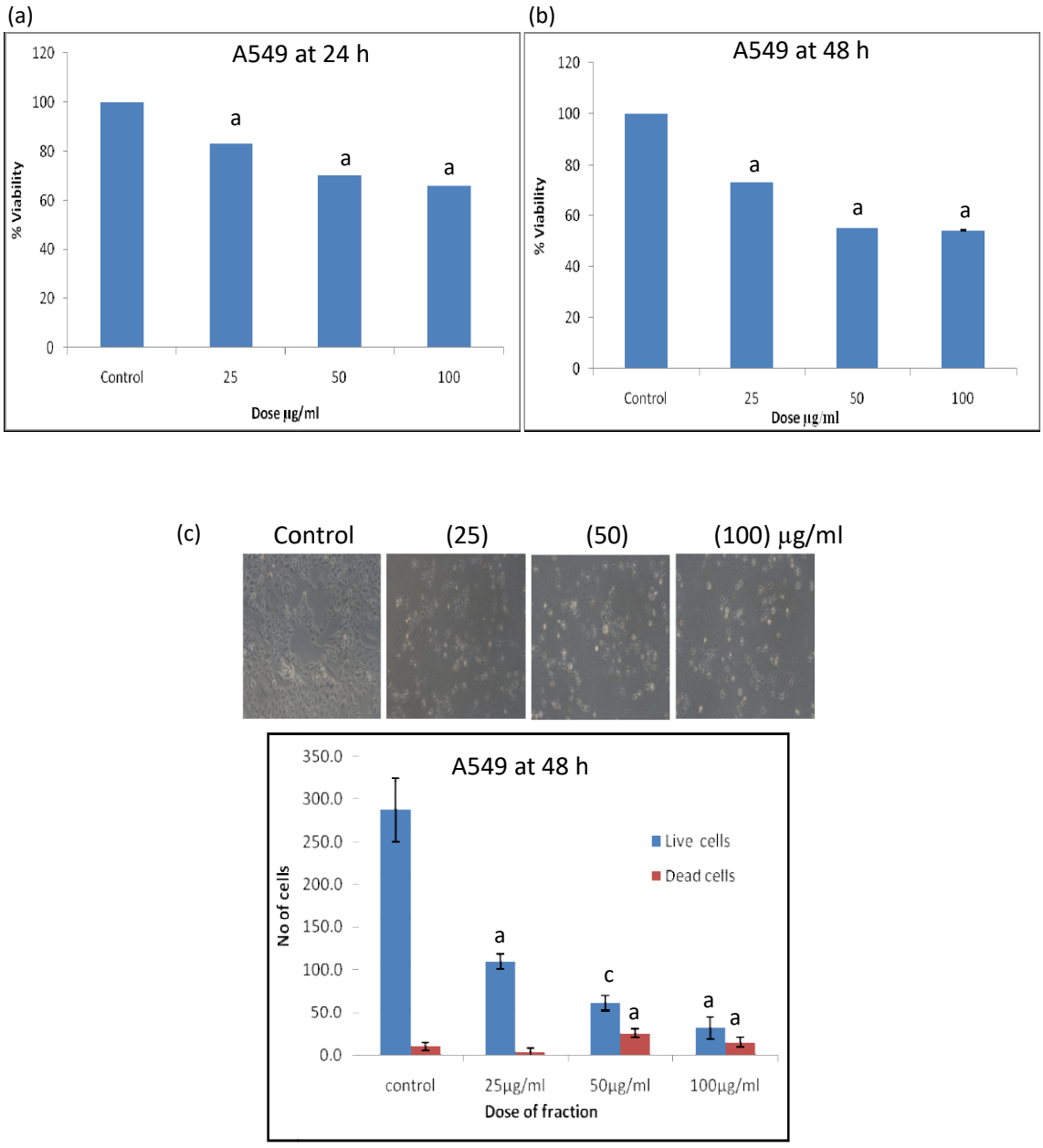

Figure 4.25: Cytotoxic effects of (a) LEX FP at 24 h and (b) LEX FP at 48 h against A549 cells, measured by MTT based method. (c) Cell counting assay of A549 cells against LEX FP measured by trypan blue dye exclusion method. The viability is calculated as % of control (100%) Values were expressed as mean ± sem; n=3. Error bars represent standard deviation [a] Significantly different ($p \leq 0.001$) against untreated control. [c] Significantly different ($p \leq 0.05$) against untreated control.

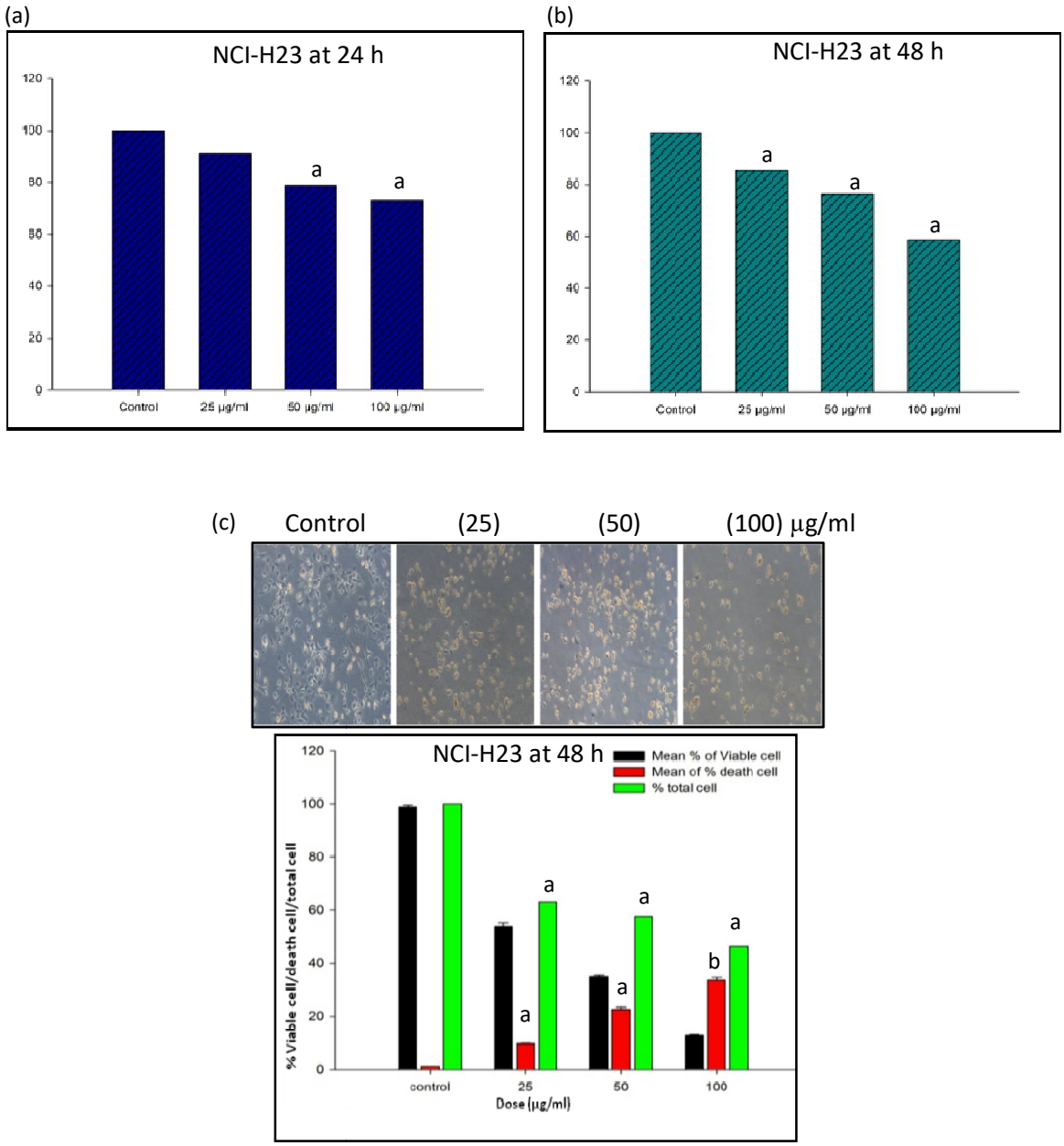

Figure 4.26: Cytotoxic effects of (a) LEX FP at 24 h and (b) LEX FP at 48 h against NCI-H23 cells, measured by MTT based method. (c) Cell counting assay of NCI-H23 cells against LEX FP measured by trypan blue dye exclusion method. The viability is calculated as % of control (100%) Values were expressed as mean ± sem; n=3. Error bars represent standard deviation [a] Significantly different ($p \leq 0.001$) against untreated control. [b] Significantly different ($p \leq 0.01$) against untreated control.

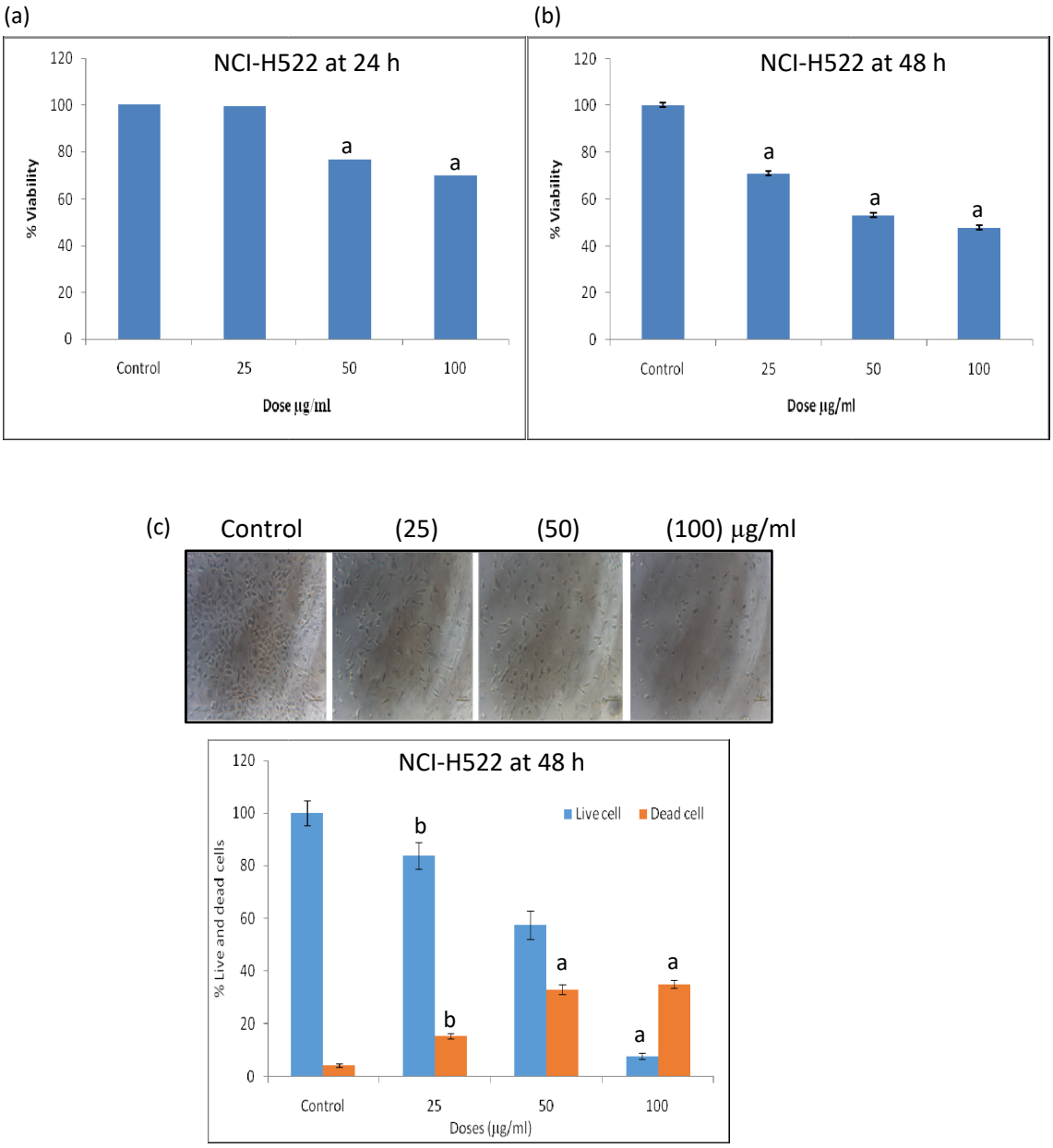

Figure 4.27: Cytotoxic effects of (a) LEX FP at 24 h and (b) LEX FP at 48 h against NCI-H522 cells, measured by MTT based method. (c) Cell counting assay of NCI-H522 cells against LEX FP measured by trypan blue dye exclusion method. The viability is calculated as % of control (100%) Values were expressed as mean ± sem; n=3. Error bars represent standard deviation [a] Significantly different ($p \leq 0.001$) against untreated control. [b] Significantly different ($p \leq 0.01$) against untreated control. [b] Significantly different ($p \leq 0.05$) against untreated control.

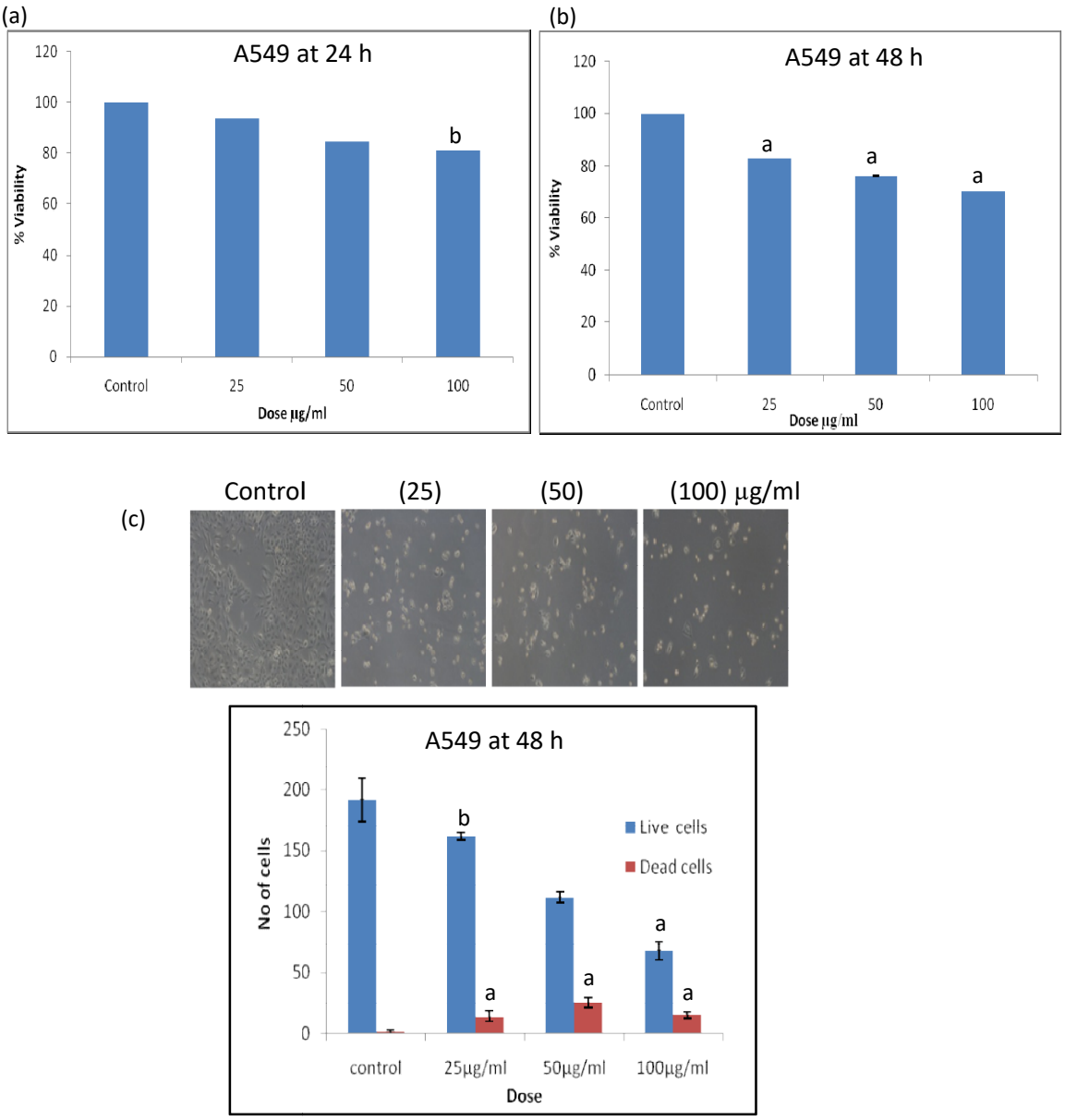

Figure 4.28: Cytotoxic effects of (a) LEX BP at 24 h and (b) LEX BP at 48 h against A549 cells, measured by MTT based method. (c) Cell counting assay of A549 cells against LEX BP measured by trypan blue dye exclusion method. The viability is calculated as % of control (100%) Values were expressed as mean ± sem; n=3. Error bars represent standard deviation [a] Significantly different ($p \leq 0.001$) against untreated control. [b] Significantly different ($p \leq 0.01$) against untreated control.

4.14. LEX free phenolic and LEX bound phenolic induced apoptosis in lung cancer cell lines detection by AO/EtBr double staining and validation by flowcytometry using Annexin V-FITC and PI

AO/EtBr dye staining was performed on lung cancer cell lines exposed with 25 µg/ml, 50 µg/ml, and 100 µg/ml of phenolic extracts of LEX to identify if the cells undergo necrosis, apoptosis, or a combination of both. Acridine Orange (AO) may readily enter the regular and initial apoptotic cells with intact membranes, and flash green fluorescence upon attaching to DNA, making it possible to detect fundamental morphological variations in apoptotic cells using the double AO/EtBr fluorescence labeling approach. Varying fluorescence is seen at various phases of apoptosis, which serves as an indicator of these processes; for example, green/yellow indicates an intact or early apoptotic cell, whereas orange indicates late apoptotic and red indicates a dead cell. Since AO/EtBr staining may be used to both qualitatively and quantitatively identify apoptosis, it is widely accepted as a reliable approach for doing so.

The degree of induced apoptosis by phenolic extracts of LEX in lung Cancer cell lines are further confirmed by flowcytometry. The treated cells were stained with Annexin V-FITC and Propidium Iodide (PI) after 48 hours of incubation with different concentration of LEX Phenolics. As during apoptosis, loss of plasma membrane integrity leads to externalization of phosphatidylserine which is selectively detected by Annexin V-FITC and o the other hand PI permeates the cell membrane and detects necrotic cells.

The exposure of LEX free and LEX bound phenolics shows induction of apoptosis in A549 cells in dose dependent manner after 48 h of treatment (Figure 4.29, 4.32). The LEX free phenolics also stimulate apoptosis in NCI-H522 cells in dose dependent manner (Figure 4.30). We could also see similar effect in NCI-H23 cells using fluorescence microscope (Figure 4.31). The percentage of late apoptotic and necrotic cells significantly increases in all three cell lines. The results of induced apoptosis detected by fluorescence microscopic is further confirmed by flowcytometry in A549, NCI-H522 cells

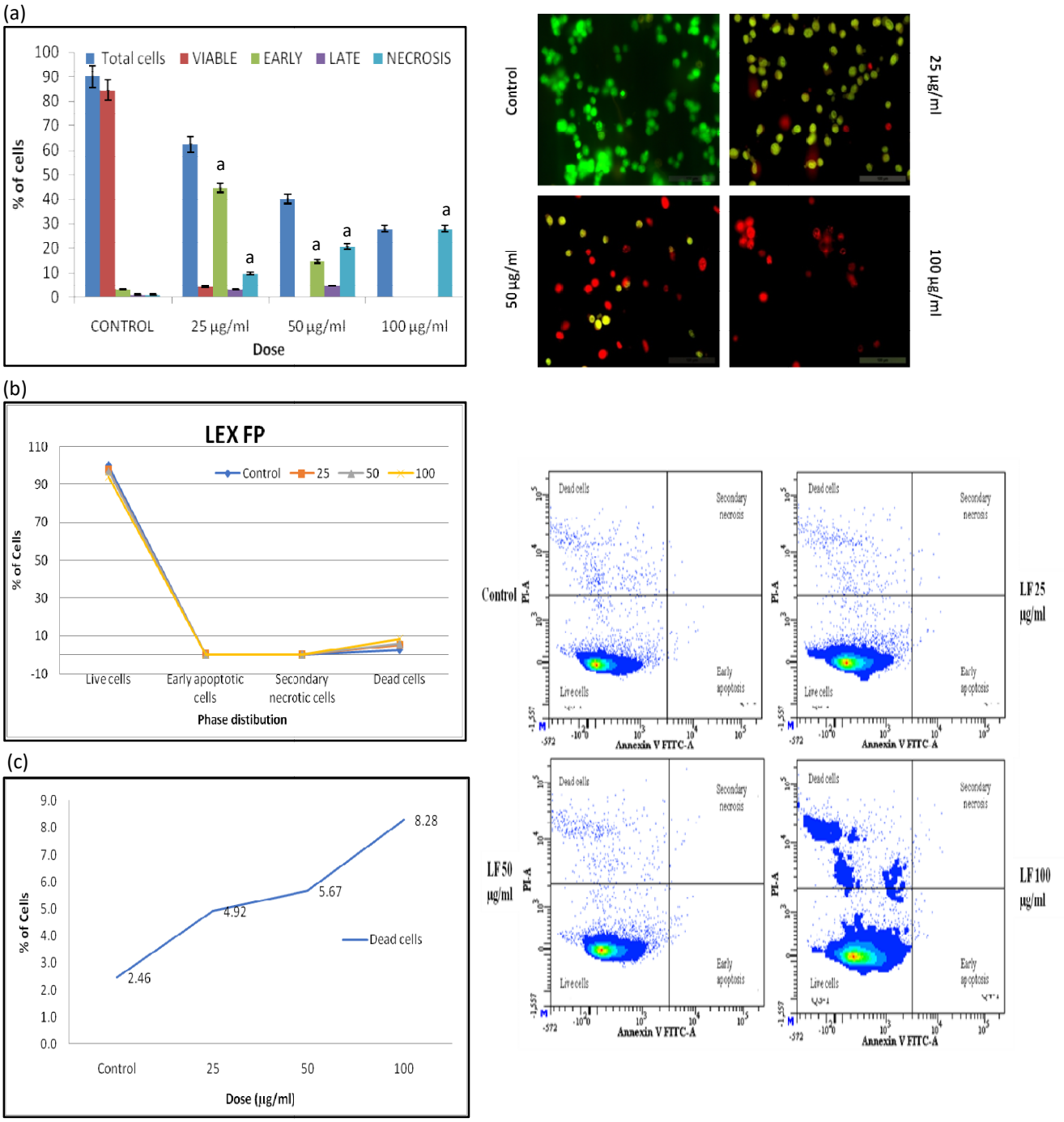

Figure 4.29: AO/EtBr staining of A549 cells treated with (a) LEX free phenolics for 48 h. The cells could be divided into viable, early apoptotic, late apoptotic and necrotic/dead cells. (b), (c) Effect of LEX free phenolics on apoptosis of A549 cell lines after 48 h of treatment. The pictorial representation of pattern of apoptosis phase distribution is shown in contour plot of Annexin V-FITC/PI for evaluation of apoptosis. Values were expressed as mean ± sem; n=3. Error bars represent standard deviation [a] Significantly different ($p \leq 0.001$) against untreated control.

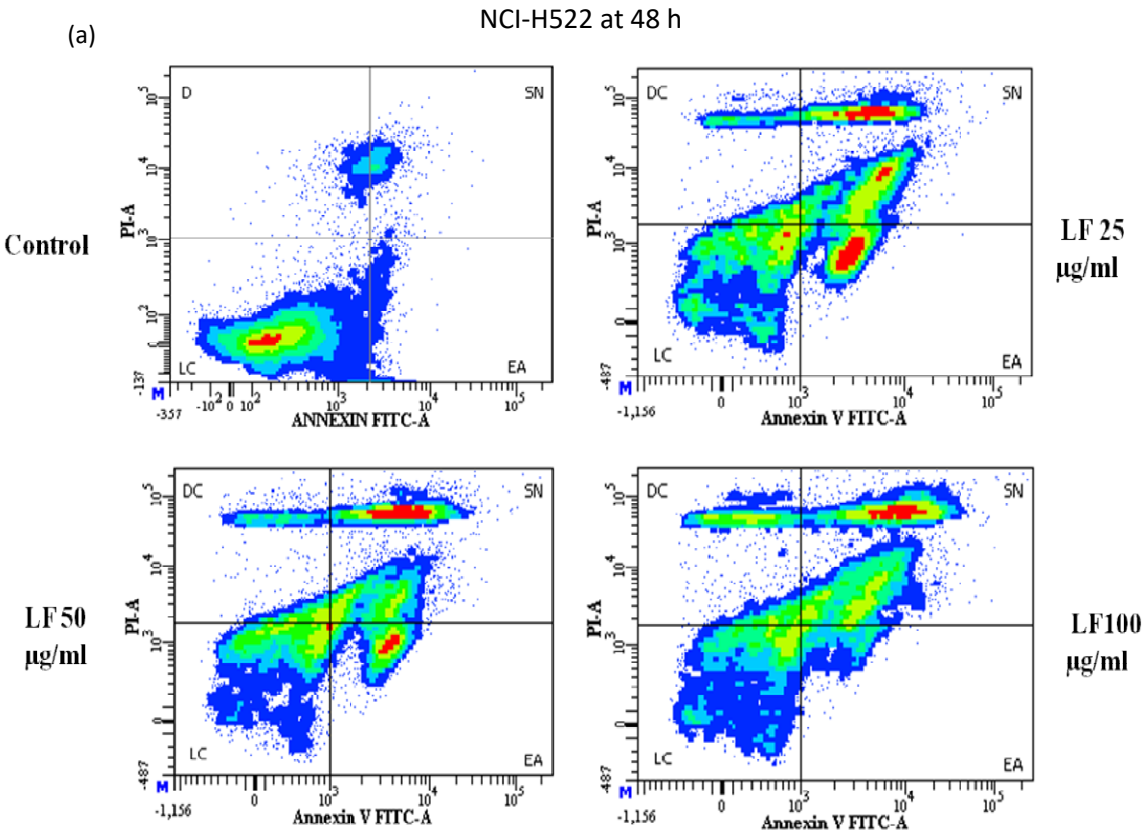

Figure 4.30: Effect of LEX free phenolics in (a) NCI-H522 cells for 48 h. The cells could be divided into viable, early apoptotic, late apoptotic and necrotic/dead cells. The pictorial representation of pattern of apoptosis phase distribution is shown in contour plot of Annexin V-FITC/PI for evaluation of apoptosis. Values were expressed as mean ± sem; n=3.

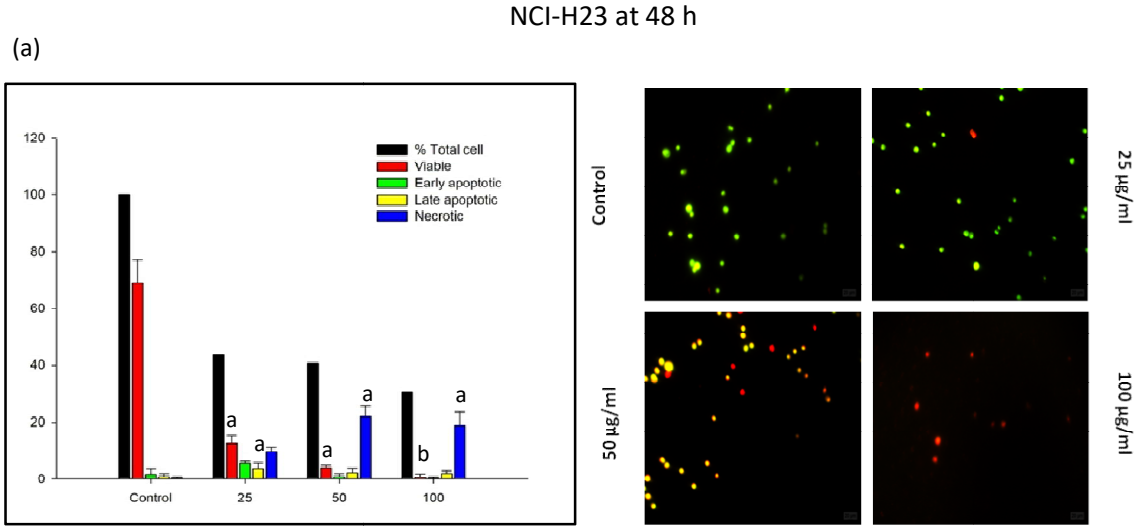

Figure 4.31: AO/EtBr staining of NCI-H23 cells treated with (a) LEX free phenolics for 48 h. The cells could be divided into viable, early apoptotic, late apoptotic and necrotic/dead cells. Values were expressed as mean ± sem; n=3. Error bars represent standard deviation [a] Significantly different ($p \leq 0.001$) against untreated control. [b] Significantly different ($p \leq 0.01$) against untreated control.

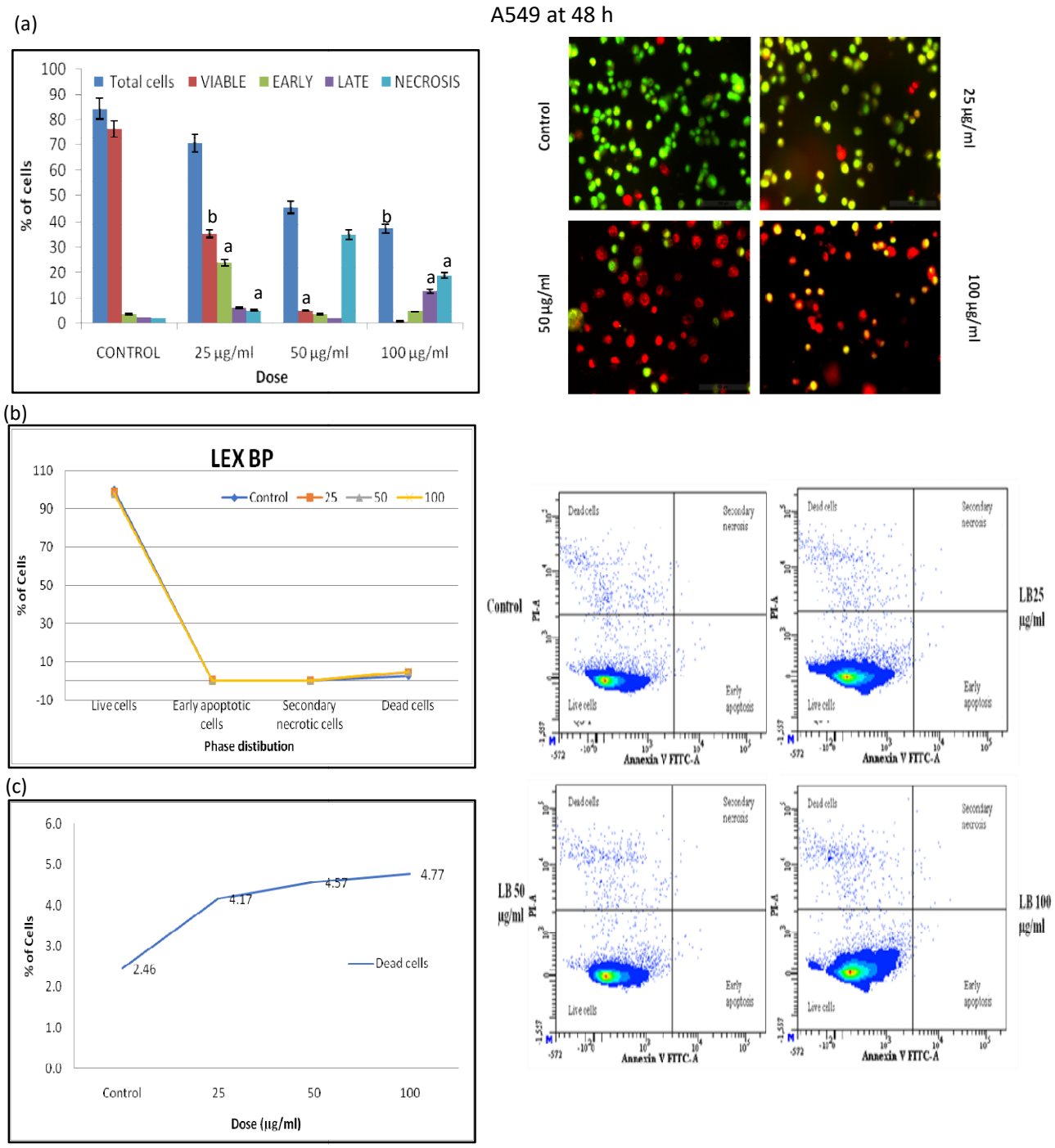

Figure 4.32: AO/EtBr staining of A549 cells treated with (a) LEX bound phenolics for 48 h. The cells could be divided into viable, early apoptotic, late apoptotic and necrotic/dead cells. (b) Effect of LEX bound phenolics on apoptosis of A549 cell lines after 48 h of treatment. The pictorial representation of pattern of apoptosis phase distribution is shown in contour plot of Annexin V-FITC/PI for evaluation of apoptosis. Values were expressed as mean ± sem; n=3. Error bars represent standard deviation [a] Significantly different ($p \leq 0.001$) against untreated control. [b] Significantly different ($p \leq 0.01$) against untreated control.

4.15. LEX free phenolic and LEX bound phenolic induced autophagy and lipid accumulation in lung cancer cell lines detection by fluorescence microscopy, flowcytometry and Oil Red O staining.

The detection and quantification of autophagosome production in lung cancer cells was done using flow cytometry as well as microscopic examination. The microscopic investigation of A549 cell lines showed that numbers of autophagic vacuoles were significantly increased in number and size of AVOs increased after 48 hours of exposure to LEX free phenolic fraction (25 µg/ml, 50 µg/ml, 100 µg/ml) compared to control cells (Figure 4.33). In case of NCI-H23 cells we have observed significant increase in numbers of autophagic vacuoles and size of AVOs after 48 hours of exposure to LEX free phenolic fraction (Figure 4.34). We further confirmed the result of induced autophagy by using flowcytometry in A549 cells. We have observed the increase in mean fluorescent intensity in treated cells indicating the percentage of fold change of acid vesicles which validates the above findings (Figure 4.33).

Further we have analyzed the lipid accumulation in response to the LEX phenolic fraction in A549 and NCI-H23 cells using Oil Red O staining (40X). Cells treated with LEX free phenolic (25 µg/ml, 50 µg/ml, 100 µg/ml) for 48 hours exhibits a lipid accumulation phenotype (Figure 4.33, 4.34). The observed significant increase in lipid accumulation in lung cancer cells indicated cellular stress induced by the plant fraction which might correlate to autophagy pathway.

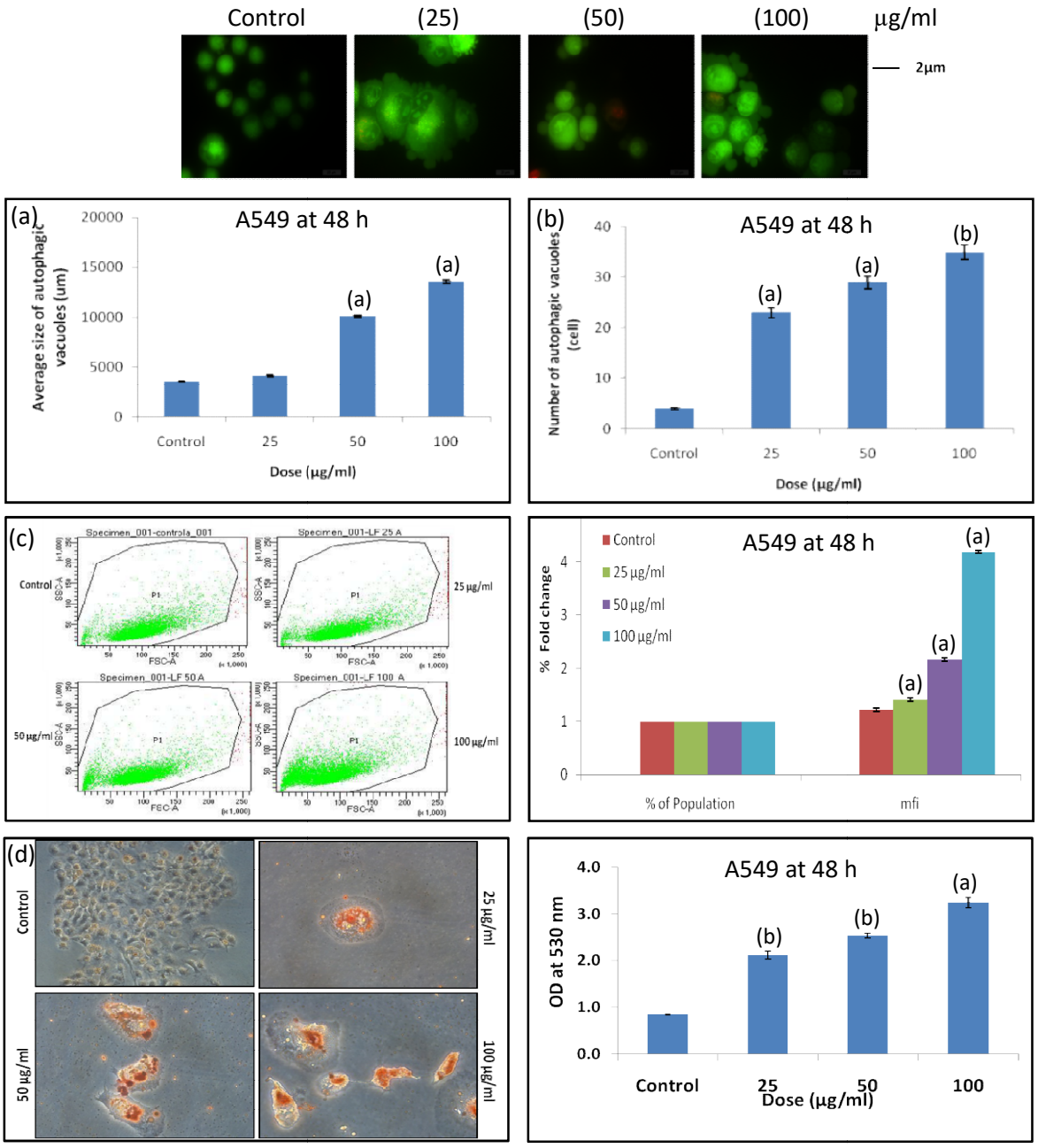

Figure 4.33: Effect of LEX FP on A549 autophagosome formation. (a) Number of autophagosome generation (b) Average size of the autophagosome (c) The data are represented in scattered plot along with bar graph depicting fold changes in vesicle formation. (d) Oil Red O staining of A549 cell lines upon LEX FP treatment for 48 h. Values were expressed as mean ± sem; n=3. Error bars represent standard deviation [a] Significantly different ($p \leq 0.001$) against untreated control. [b] Significantly different ($p \leq 0.01$) against untreated control

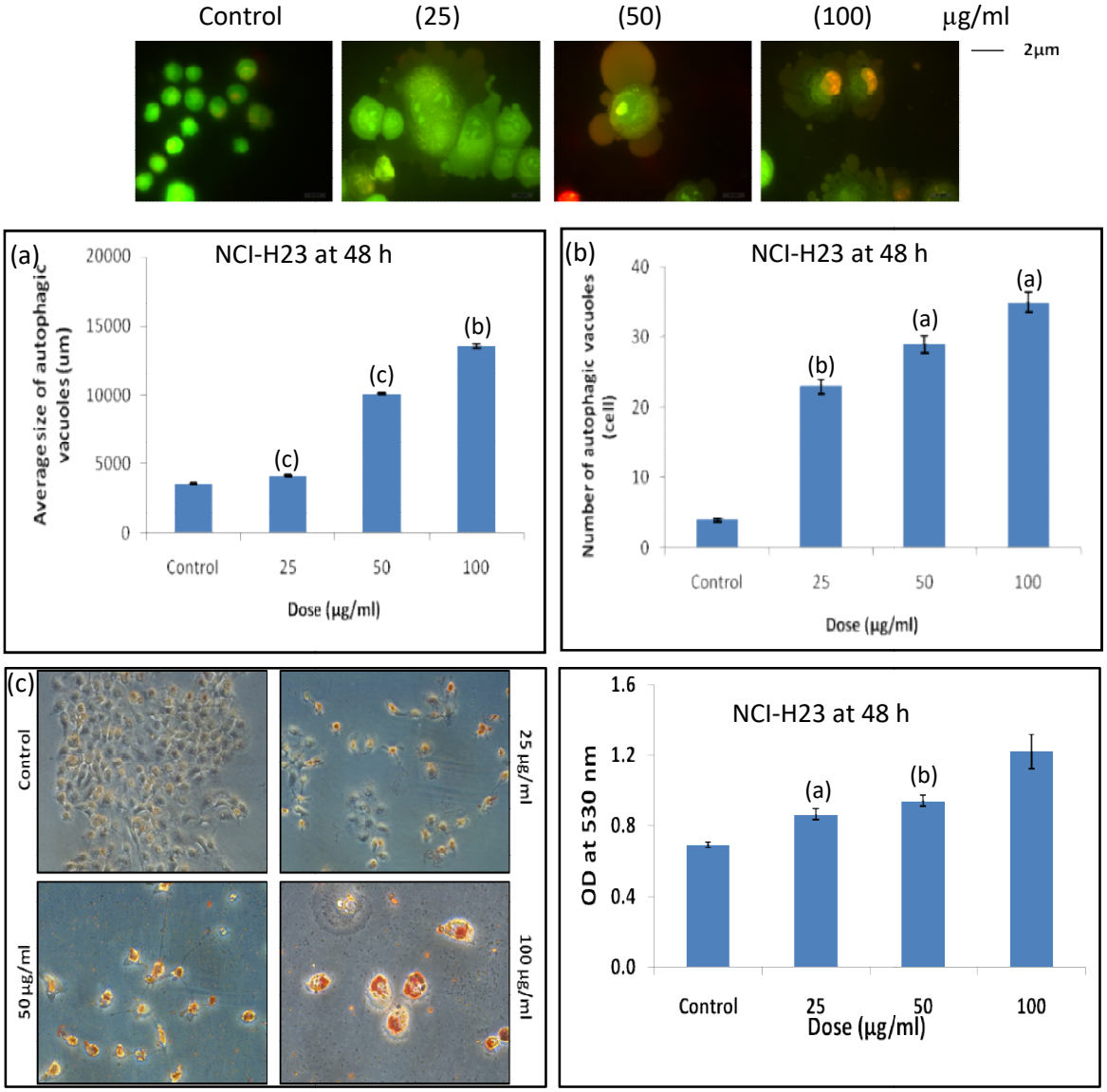

Figure 4.34: Effect of LEX FP on NCI-H23 autophagosome formation. (a) Average size of the autophagosome (b) Number of autophagosome generation (c) Oil Red O staining of NCI-H23 cell lines upon LEX FP treatment for 48 h. Values were expressed as mean ± sem; n=3. Error bars represent standard deviation [a] Significantly different ($p \leq 0.001$) against untreated control. [b] Significantly different ($p \leq 0.01$) against untreated control. [c] Significantly different ($p \leq 0.05$) against untreated control.

4.16. Effect of LEX free phenolic and LEX bound phenolic in intracellular ROS and MMP generation detected by flow cytometry

In this section, we have used flowcytometry with DCFDA-FITC-A and Rhodamine-123 to evaluate the propensity of LEX free phenolic and LEX bound phenolic fraction (25 µg/ml, 50 µg/ml, 100 µg/ml) to produce intracellular ROS and MMP in the exposed lung cancer cell lines. The degree of fluorescence by oxidized DCF is measured after LEX phenolics treatment. Diminished fluorescence in the presence of Rhodamine-123, a fluorescent dye used to evaluate mitochondrial membrane integrity or mitochondrial membrane depolarization, represented the loss of the MMP.

We have observed a significant increase in intracellular ROS level in A549 cells as the mean fluorescence intensity increases after 48 hours of LEX free phenolic fraction exposure.. The result demonstrates that the treated A549 cell line there is an increase in number of ROS-positive cells relative to untreated cells by 2.8 ($p \leq 0.001$) folds. Also the MMP level was significantly decreased by 0.76 folds in compared to control (Figure 4.35). On the other hand the A549 cell lines, the ROS level increased by 1.25 ($p \leq 0.001$) folds and MMP fold change decreased in dose dependent manner from 0.88 to 0.73 ($p \leq 0.001$) when treated with LEX bound phenolic fraction for 48 (Figure 4.36).

Hence the LEX free and LEX bound phenolics treated cancer cells exhibit increase in intracellular ROS levels indicated by increase in mean fluorescent intensity thus resulted in mitochondrial dysfunction. The finding is supported by decrease in mitochondrial membrane potential and/or hyper polarization with increase in dose of the extract. This indicates that the phenolics treated cells undergo cellular stress and overall cell death in cancer cells either by apoptosis or autophagy,

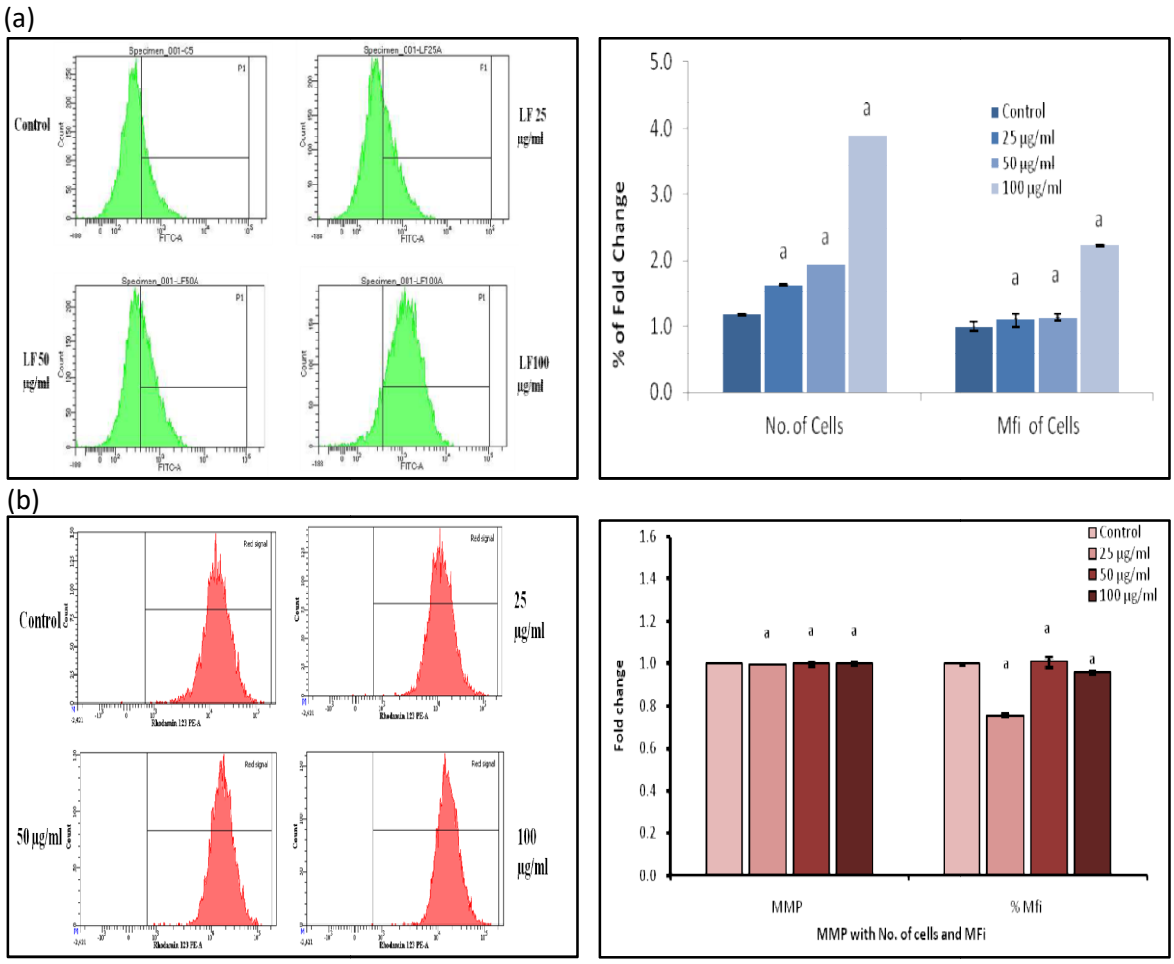

Figure 4.35: Effect of LEX free phenolics on (a) intracellular ROS generation of A549 cells upon treatment for 48 h. The histogram and corresponding bar graph represents the fold change in ROS generation after 48 h of plant fraction treatment. (b) Mitochondrial membrane potential of A549 cells. The histogram and corresponding bar graph represents the fold change in MMP after 48 h of plant fraction treatment. Values were expressed as mean ± sem; n=3. Error bars represent standard deviation [a] Significantly different ($p \leq 0.001$) against untreated control

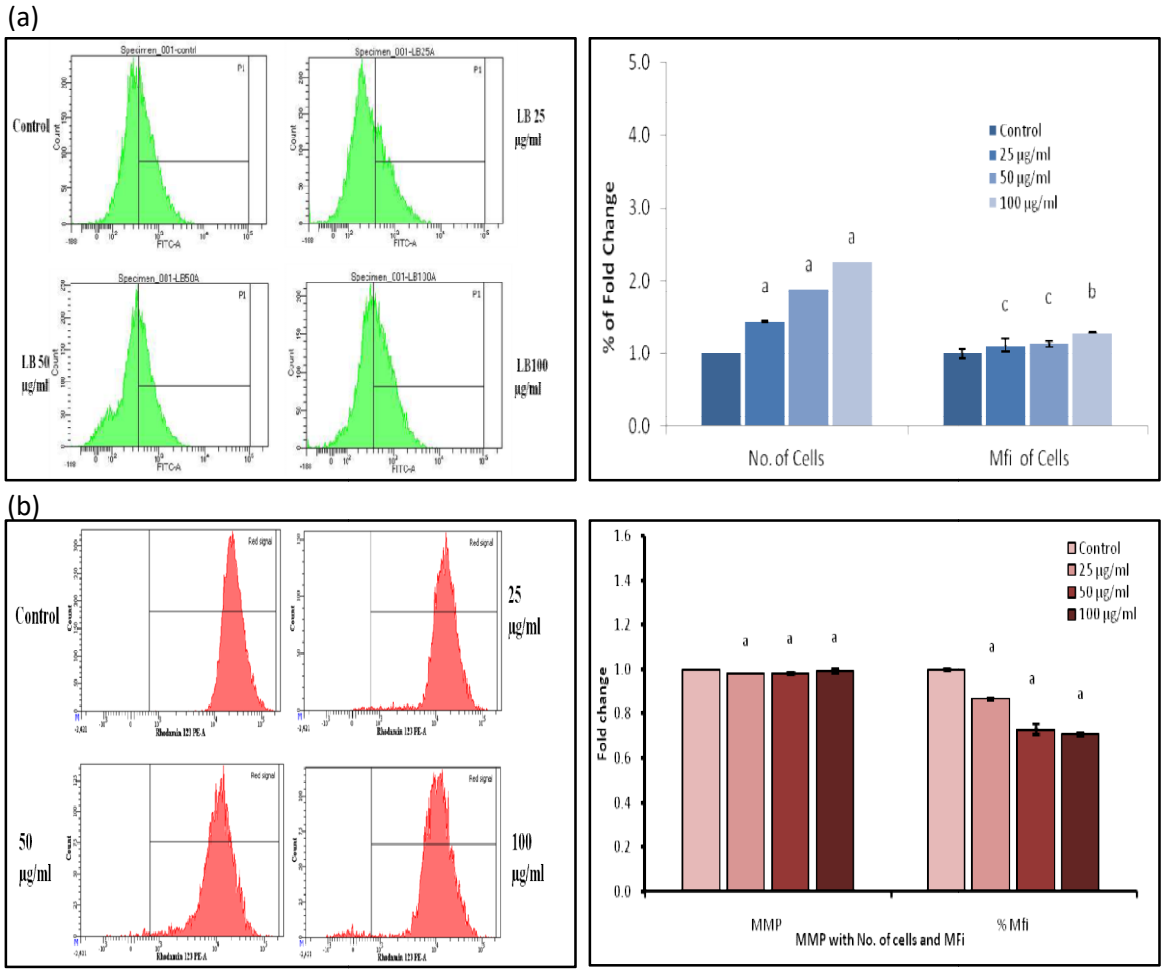

Figure 4.36: Effect of LEX bound phenolics on (a) intracellular ROS generation of A549 cells upon treatment for 48 h. The histogram and corresponding bar graph represents the fold change in ROS generation after 48 h of plant fraction treatment. (b) Mitochondrial membrane potential of A549 cells. The histogram and corresponding bar graph represents the fold change in MMP after 48 h of plant fraction treatment. Values were expressed as mean ± sem; n=3. Error bars represent standard deviation [a] Significantly different ($p \leq 0.001$) against untreated control. [b] Significantly different ($p \leq 0.01$) against untreated control. [c] Significantly different ($p \leq 0.05$) against untreated control.

4.17. Cell cycle analysis in lung cancer cell lines using LEX free phenolic and LEX bound phenolic

As most of the known anticancer drugs act by altering cell cycle distribution of cancer cells at G0/G1, S, G2/M phase and leading to cell death or apoptosis. We have investigated the effect of LEX free and LEX bound phenolic fractions in cell cycle phase distribution in lung cancer cell lines by quantifying the DNA content using Propidium Iodide (PI) fluorescence in flowcytometer.

We have observed a significant increase in A549 cell population at S and G2/M phase after 48 hours when exposed to LEX free phenolics (25 µg/ml, 50 µg/ml, 100 µg/ml) (Figure 4.37). The population of the treated cells was arrested in S phase up to 82% ($p \leq 0.01$) with respect to the control cells 14.35% ($p \leq 0.001$). A considerable increase in the S-Phase and G2/M cell population was observed after 48 hours of treatment with LEX free phenolic in NCI-H522 cells. The cells were arrested at S phase by 37.6% ($p \leq 0.001$) and at G2/M phase by 13.75% ($p \leq 0.001$) with respect to the control 20.4% ($p \leq 0.001$) (Figure 4.37). The cell population in both A549 and NCI-H522 cell lines undergoes apoptosis by 5.5-13.75% ($p \leq 0.01$) with respect to control.

A549 cells exposed to 25 µg/ml, 50 µg/ml, and 100 µg/ml of LEX bound phenolic extract showed a considerable increase in cell population and arrest at the S phase by 24.8% ($p \leq 0.01$) and at G2/M phase by 28.15% ($p \leq 0.05$) with respect to the control 14.35% and 8.55% respectively at 48 hours (Figure 4.38). Similar to the LEX free phenolics action in A549 cells the LEX bound phenolics treated cells undergoes apoptosis by 5.5% ($p \leq 0.001$) compared to the control.

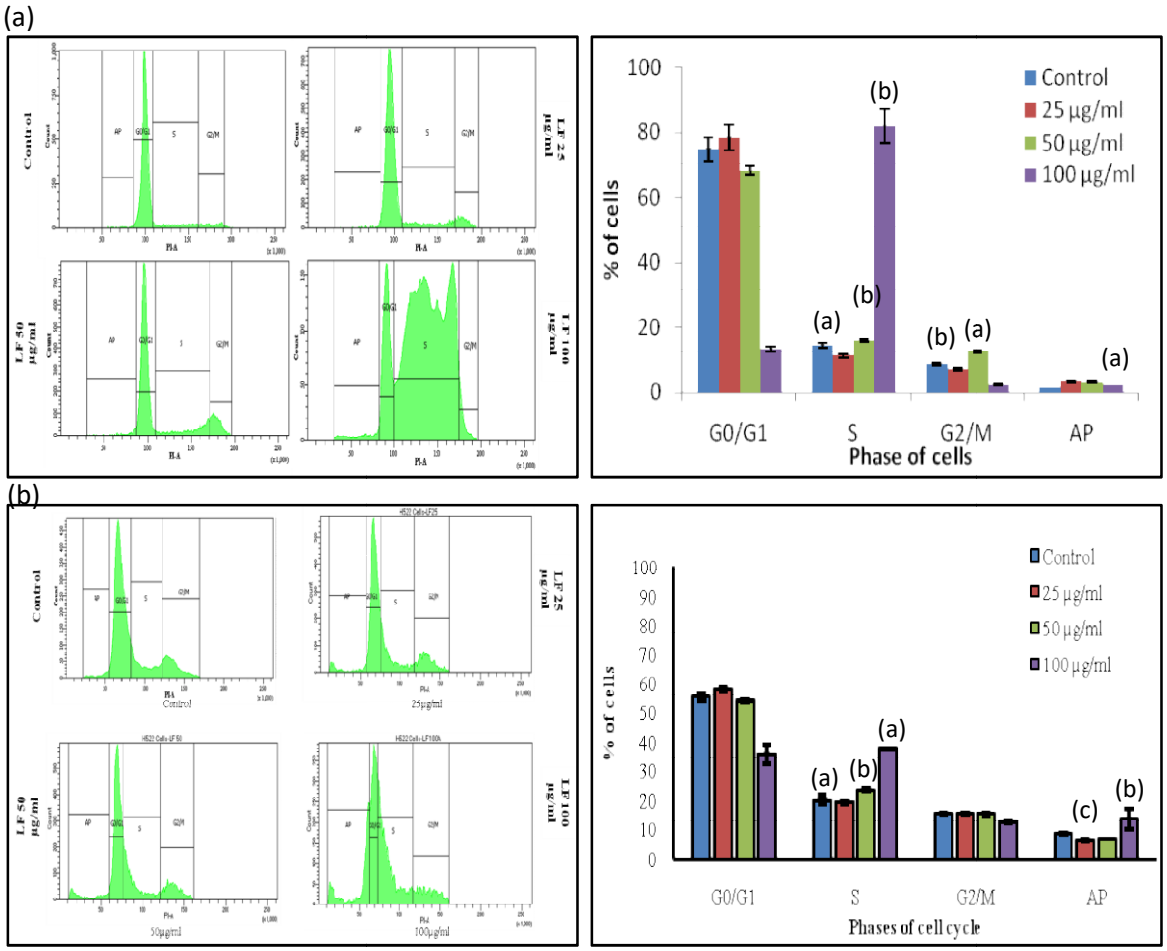

Figure 4.37: Effect of LEX free phenolics on cell cycle distribution of (a) A549 cells and (b) NCI-H522 cells after 48 h of incubation. Histogram display of DNA content (x-axis, PI-fluorescence) vs. cell count (y-axis) and bar graph representation of cell cycle distribution at G0/G1, S and G2/M phase. Values were expressed as mean ± sem; n=3. Error bars represent standard deviation [a] Significantly different ($p \leq 0.001$) against untreated control. [b] Significantly different ($p \leq 0.01$) against untreated control. [c] Significantly different ($p \leq 0.05$) against untreated control.

(a)

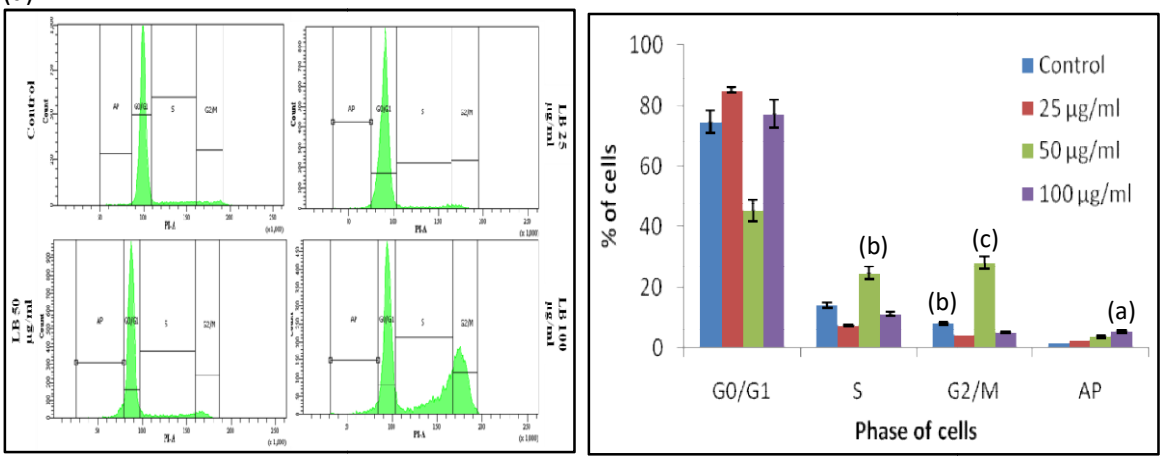

Figure 4.38: Effect of (a) LEX bound phenolics on cell cycle distribution of A549 cells after 48 h of incubation. Histogram display of DNA content (x-axis, PI-fluorescence) vs. cell count (y-axis) and bar graph representation of cell cycle distribution at G0/G1, S and G2/M phase. Values were expressed as mean ± sem; n=3. Error bars represent standard deviation [a] Significantly different ($p \leq 0.001$) against untreated control. [b] Significantly different ($p \leq 0.01$) against untreated control.

4.18. Effect of Lex Free Phenolic and Bound Phenolic in cell proliferation of lung cancer cell lines using CFSE labeled flowcytometry

The effect of LEX free and LEX bound phenolics in overall lung cancer cell proliferation was monitored using intracellular dye, carboxylfluorescein succininmidyl ester (CFSE) in flowcytometry. As with each cell division, the fluorescent dye distributes throughout the daughter cells causing a drop in fluorescence intensity in proliferating cells is therefore measured by flowcytometry.

The exposure of A549 cells with LEX free phenolic fractions for 72 hours shows significant reduction in cell proliferation up to 29.16% ($p \leq 0.001$) with respect to the control. The rate of proliferation was decreased by 15.6% ($p \leq 0.01$) in case of LEX bound phenolics treatment in A549 cells (Figure 4.39). Interestingly the proliferation rate of human PBMCs was increased in dose dependent manner upon exposure to either phenolic fractions of LEX (Figure 4.40). This observation corresponds to the cell viability of LEX phenolic fractions measured by MTT based method (Figure 4.24). Thus from the findings we can conclude that the plant phenolic fractions inhibiting overall cell proliferation in lung cancer cell lines in dose dependent manner and on the other hand enhances cell proliferation in human PBMCs.

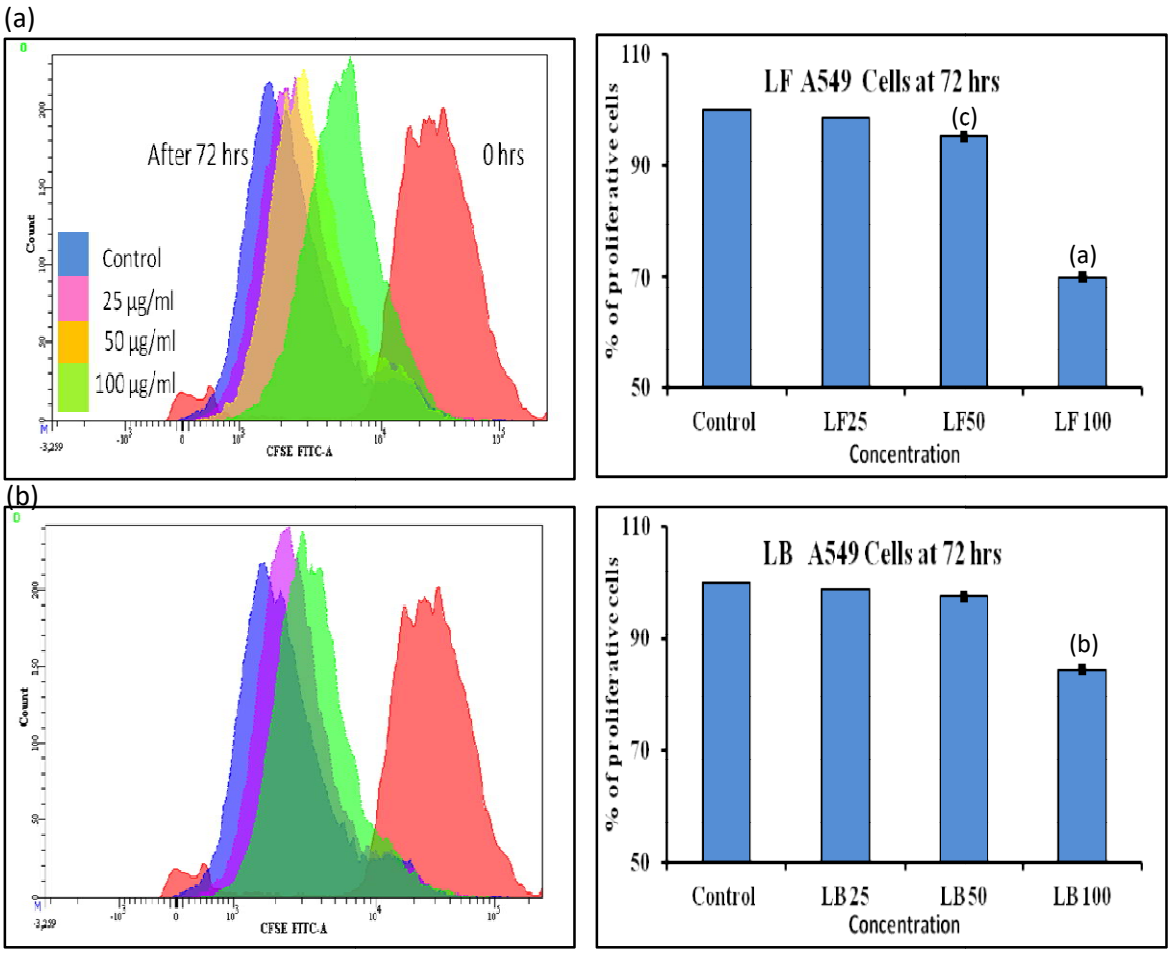

Figure 4.39: Effect of LEX free and bound phenolics on cell proliferation of CFSE labelled lung cancer cell lines incubated with 0-100µg/ml for 72 h; (a) LEX free phenolics in A549 cells (b) LEX bound phenolics in A549 cells. The CFSE labelled cells at 0 h were negative control. The reduction of CFSE fluorescence was measured by flow cytometry at 72 h. Values were expressed as mean ± sem; n=3. Error bars represent standard deviation [a] Significantly different ($p \leq 0.001$) against untreated control. [b] Significantly different ($p \leq 0.01$) against untreated control. [c] Significantly different ($p \leq 0.05$) against untreated control.

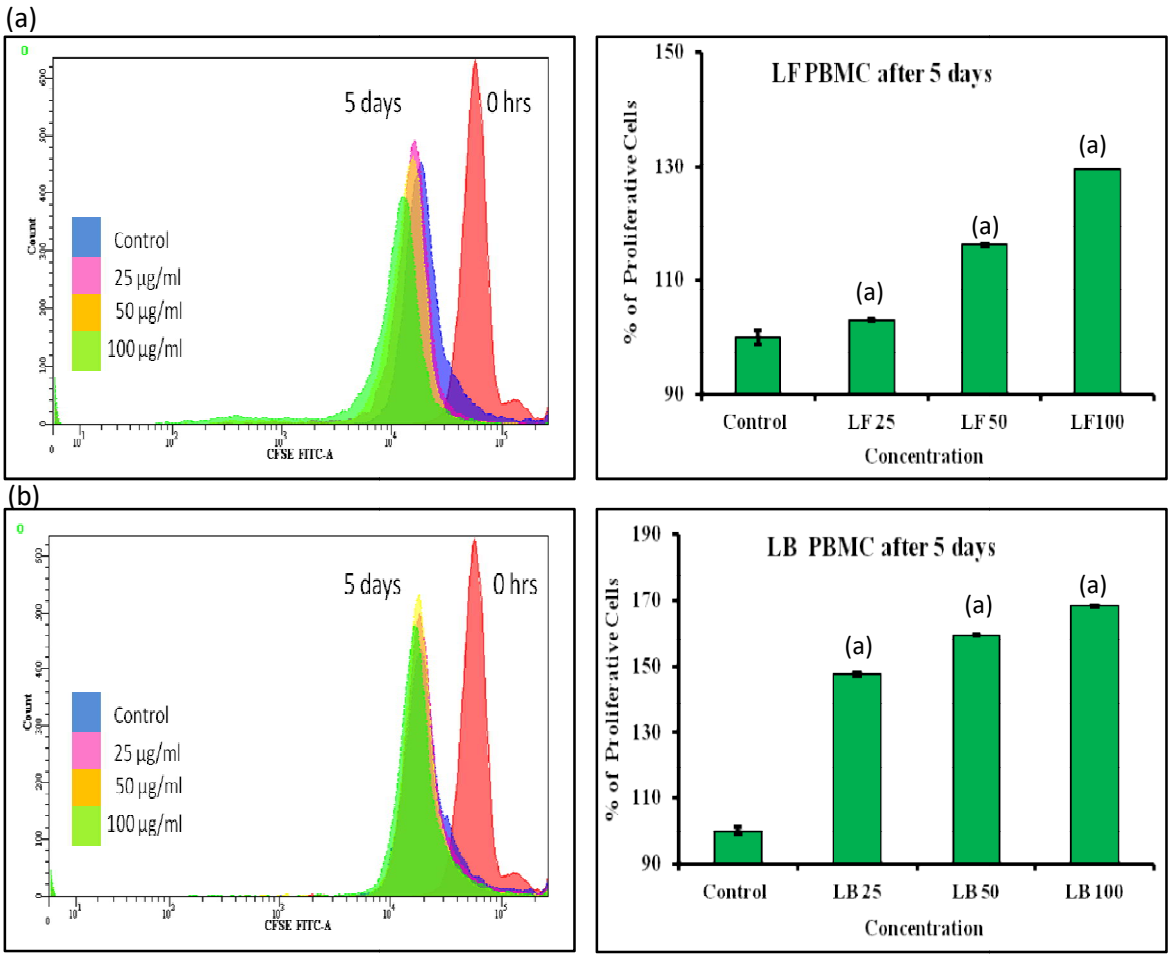

Figure 4.40: Effect of LEX phenolics on cell proliferation of CFSE labelled PBMCs incubated with 0-100µg/ml for 120 h; (a) LEX free phenolics in human PBMCs for 5 days (b) LEX bound phenolics in human PBMCs for 5 days. The CFSE labelled cells at 0 h were negative control. The reduction of CFSE fluorescence was measured by flow cytometry at 120 h. Values were expressed as mean ± sem; n=3. Error bars represent standard deviation [a] Significantly different ($p \leq 0.001$) against untreated control.

4.19. The effect of Lex free phenolic and LEX bound phenolic fractions in clonogenic and cell migration ability in lung cancer cell lines

Cell migration and colony formation is an essential cellular behavior of cancer cells that plays a crucial role in disease aggressiveness and metastasis. Therefore, reducing this clonogenic and migratory potential of cancer cells is essential for both successful lung cancer eradication and disease prevention. This motivated to study the inhibitory effect LEX free phenolic and LEX bound phenolic fractions in colony formation and cell migration in lung cancer cell lines.

The lung cancer cells, A549 and NCI-H23, the clonogenicity was significantly inhibited in dose dependent manner as well as the rate of migration was subdued remarkably in dose dependent manner (25 µg/ml, 50 µg/ml, 100 µg/ml) when exposed to LEX free phenolics for 48 hours (Figure 4.41). The clonogenicity of A549 cells were remarkably reduced to 35% and migratory efficacy is inhibited up to 20% when treated with LEX free phenolics. Likewise, in NCI-H23 cells, the clonogenicity is reduced to less than 5% and the rate of migration is significantly inhibited when treated with LEX free phenolics. The LEX bound phenolics also reduced the clonogenicity and migratory effect of A549 cell lines in done dependent manner after 48 hours of exposure (Figure 4.42). The clonogenicity of A549 cells are inhibited up to 38% and migratory efficacy is reduced to 8% when exposed to LEX bound phenolics respectively. The data suggest that LEX free and LEX bound phenolics have significantly reduced cell migration without the confounding influence of cell proliferation.

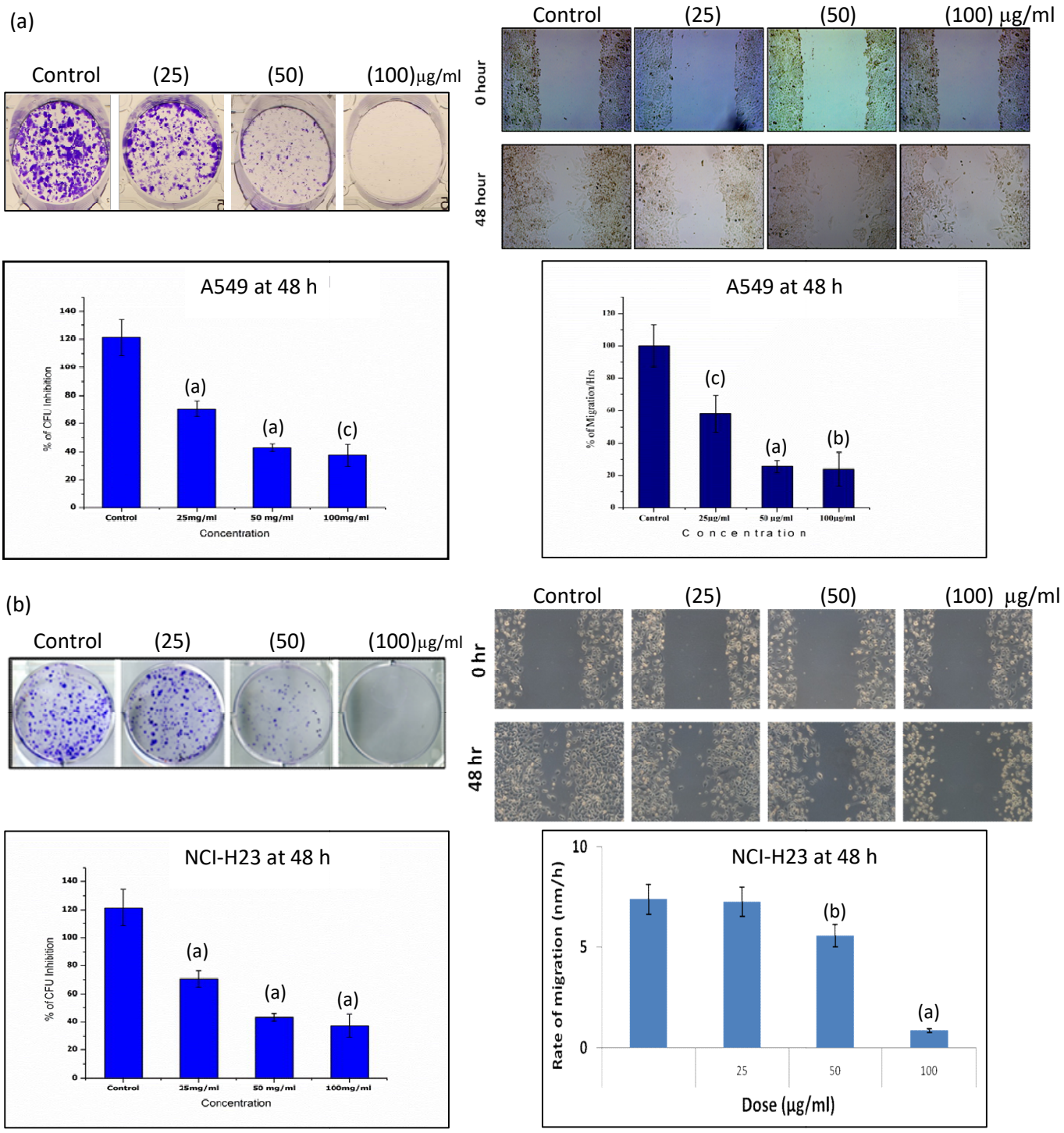

Figure 4.41: Effect of LEX free phenolics on (a) Clonogenic assay and cell migration in A549 cell lines; (b) Clonogenic assay and cell migration in NCI-H23 cell lines. Values were expressed as mean ± sem; n=3. Error bars represent standard deviation [a] Significantly different ($p \leq 0.001$) against untreated control. [b] Significantly different ($p \leq 0.01$) against untreated control. [c] Significantly different ($p \leq 0.05$) against untreated control

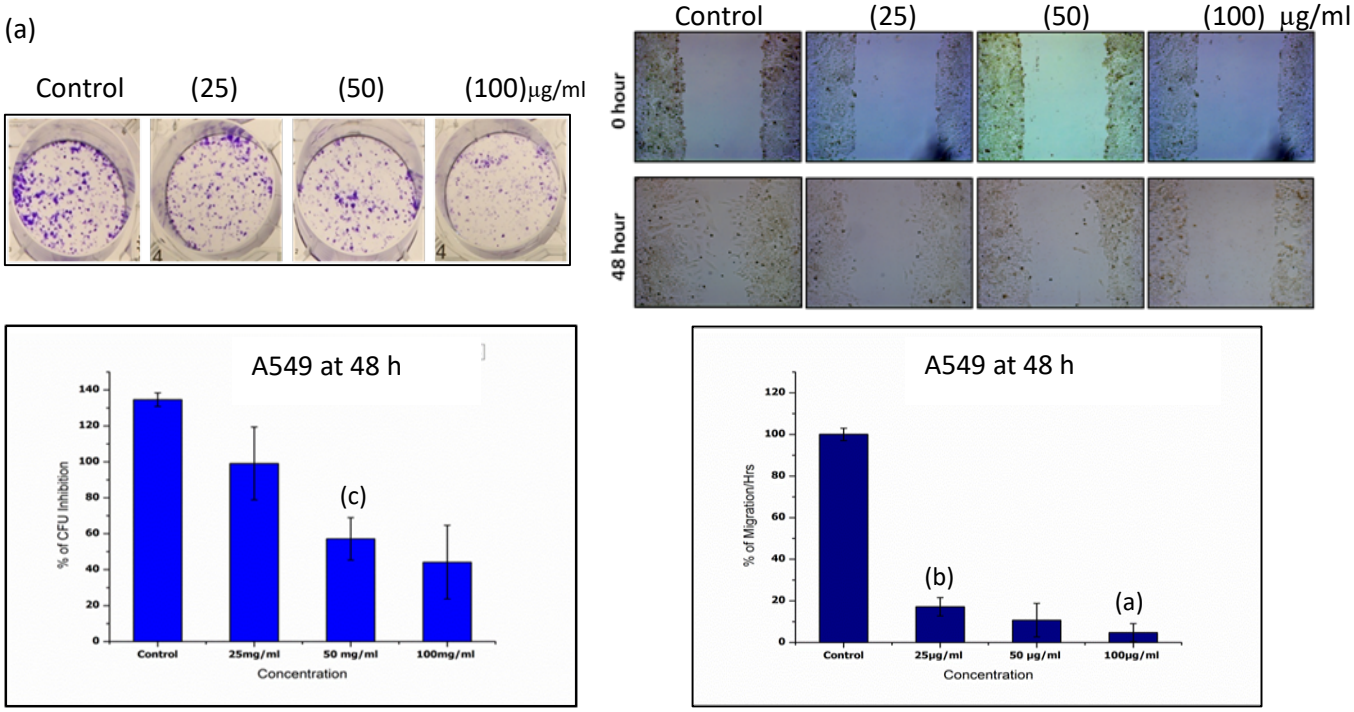

Figure 4.42: Effect of LEX bound phenolics on (a) Clonogenic assay and (b) cell migration in A549 cell lines. Values were expressed as mean ± sem; n=3. Error bars represent standard deviation [a] Significantly different ($p \leq 0.001$) against untreated control. [b] Significantly different ($p \leq 0.01$) against untreated control. [c] Significantly different ($p \leq 0.05$) against untreated control.

4.20. OHRLCMS chromatogram results for LEX free phenolic compound

A composite mixture of known anticancer phytochemicals along with some unknown molecular peaks present in the fraction that may have acted over anticancer efficacy against lung cancer. The major compounds in free phenolic fraction include Resorcinol, Resperpine, Trolox, Soyasaponin 1, 6-Gingerol, Xylitol, Rhamnetin, Robinetin, etc (Table 4.5).

OHRLCMS chromatogram of methanolic extract of LEX free phenolic compound are shown in Figure 4.43.

Table 4.5: Anticancer activity of bioactive compounds found in LEX polyphenols.

Compound	Plant source	Inhibition of Cancer
Resorcinol	*Myristica fatua* Houtt	Lung, Liver, Pancreas
Resperpine	*Rauwolfia vomitoria*	Lung, Ovary, Breast
Trolox	*Rutaceae* family	Breast, Ovary, Colon
Soyasaponin 1	*Glycine max*	Lung, Colon, Osteosarcoma
6-Gingerol	*Zingiberaceae* family	Lung, Leukemia, Breast
Xylitol	*Betulaceae* family	Lung, Oral, Pancreas,
Rhamnetin	*Syzygium aromaticum*	Lung, Breast, Liver
Robinetin	*Acacia mearnsii*	Colon, Breast, Liver

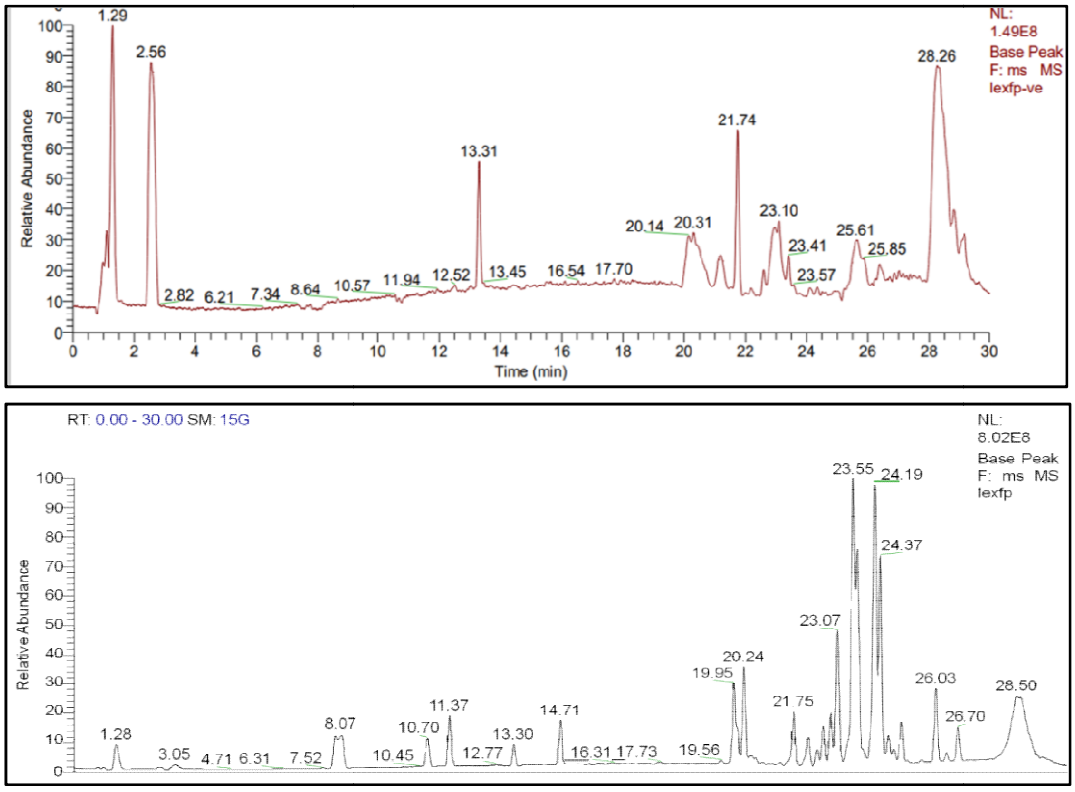

Figure 4.43: OHRLCMS chromatogram of methanolic extract of LEX free phenolic compound

4.21. Toxicity of LEX free phenolics in Balb/C mice.

The treatment of LEX free phenolics to Balb/C mice did not cause any toxicity and mortality. The plant phenolics did not alter the test results of hepatotoxicity, nephtotoxicity and hematological parameters as shown in Table 4.6, Table 4.7 and Table 4.8.

Table 4.6: Balb /C mice test result for hepatotoxicity parameters

	Total Protein (g/dL)	Albumin (g/dL)	AST (U/L)	ALT (U/L)	ALKP (U/L)	Total Bilirubin (mg/dL)	Unconj. Bilirubin (mg/dL)	Direct Bilirubin (mg/dL)	Glucose (mg/dL)
Control	**5.67 ± 0.19**	**2.88 ± 0.11**	**129.50 ± 40.19**	**32.50 ± 10.29**	**133.17 ± 21.12**	**0.85 ± 0.24**	**0.05 ± 0.04**	**0.81 ± 0.20**	**125.00 ± 9.57**
Lex FP (100 mg/kg body. wt)	**6.22 ± 0.41**	**3.28 ± 0.27**	**109.50 ± 23.75**	**38.83 ± 6.15**	**132.67 ± 27.78**	**1.18 ± 0.27**	**0.01 ± 0.03**	**1.17 ± 0.27**	**100.33 ± 13.41**

Table 4.7: Balb /C mice test result for nephrotoxicity parameters.

	BUN (mg/dL)	Creatinin (mg/dL)	Sodium (mmol/L)	Potassium (mmol/L)
Control	**14.92 ± 3.57**	**0.10 ± 0.02**	**157.17 ± 1.47**	**6.82 ± 0.63**
Lex FP (100 mg/kg body. wt)	**16.47 ± 1.38**	**0.07 ± 0.02**	**160.83 ± 2.40**	**6.35 ± 0.66**

Table 4.8: Balb/C mice test result of hematological parameters

Parameters (Unit)	**Control**	**Lex FP**
WBC(m/mm^3)	5.85±1.65	4.89±0.52
Lymphocytes (%)	82.42±3.74	78.6±5.71
Monocytes (%)	2.53±0.16	1.98±0.50
Neutrophils (%)	10.68±2.94	12.8±3.07
Eosinophils (%)	3.5±1.38	5.85±3.71
Basophils (%)	0.3±0.09	0.72±1.02
Total RBC(m/mm^3)	9.02±0.30	9.15±0.58
MCV (fl)	49.13±1.21	50.3±1.02
HCt(%)	44.32±1.87	46.02±2.84
MCH (pg)	15.38±0.33	15.43±0.61
MCHC(g/dl)	31.3±0.39	30.98±1.10
RDW	12.78±0.44	13.35±0.42
Hb(g/dl)	13.87±0.52	14.25±0.82
MPV (fl)	7±0.26	7.17±0.52
PCt(%)	0.80±0.16	0.76±0.08

4.22. Effect of LEX free phenolics against A549 induced cancer in athymic nude mice.

In the present study we have done a pilot study in athymic nude mice to understand the antitumor activity of LEX free phenolics against A549 induced carcinoma. Interestingly the findings suggest that the tumour burden in phenolic treated groups was 29% and the tumourigenicity was significantly inhibited up to 71% with respect to the control. We have observed that antitumor activity of LEX free phenolic fraction is significantly higher than the CAN free phenolic fractions. Survival/mortality rate is to be kept in mind before doing the experiments for significance of the results.

(a)

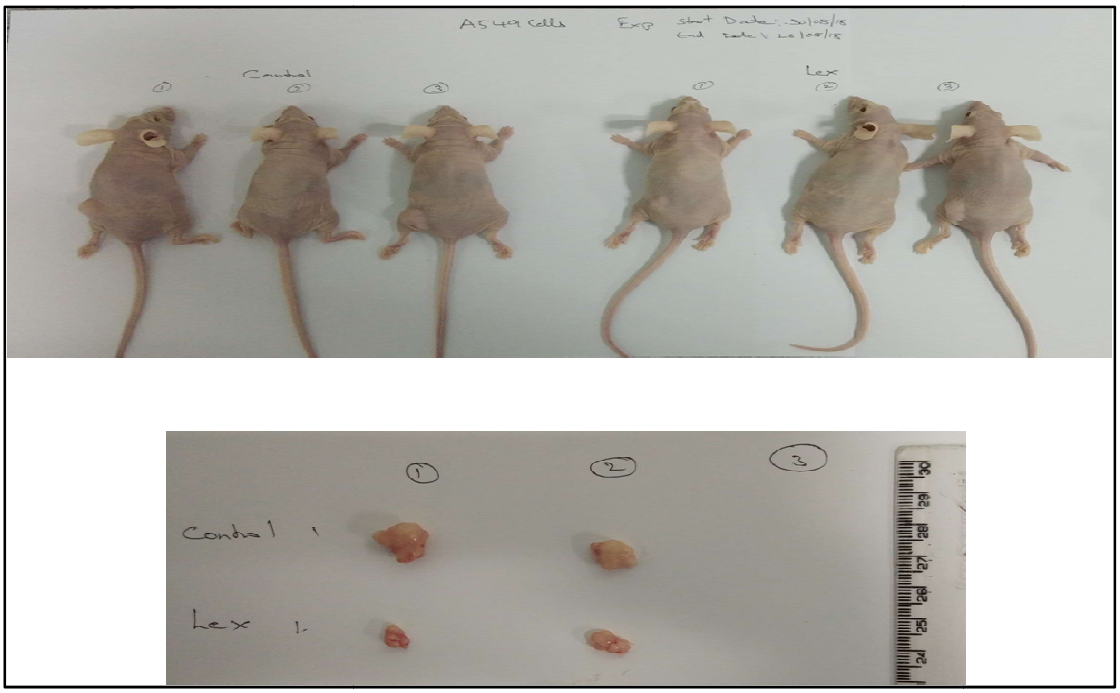

(b)

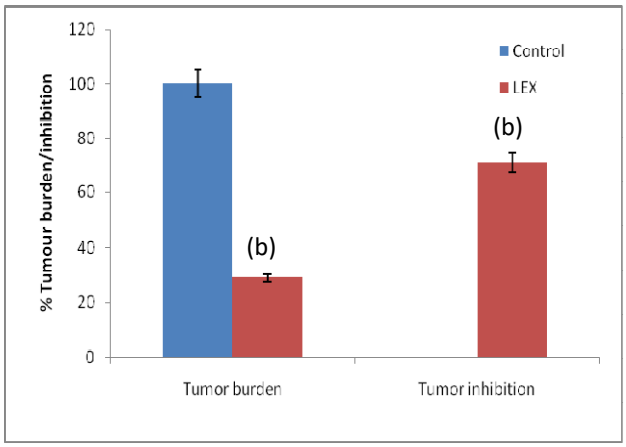

Figure 4.44: Effect of LEX free phenolics on (a) athymic nude mice against A549 induced carcinoma. (b) Bar graph represents the % tumour burden and inhibition. Values were expressed as mean ± sem; Error bars represent standard deviation. [b] Significantly different ($p \leq 0.01$) against untreated control.

Based on the our findings, the free and bound phenolic fractions extracted from the leaves of *Etlingera linguiformis* (CAN) of the Zingiberaceae family and *Smilax ovalifolia* (LEX) of the Smilacaceae family exhibit strong anti-proliferative and pro-apoptotic activity against human lung cancer cell lines A549, NCI-H522, and NCI-H23. The two plants have long histories of traditional usage in folk medicine and lifestyle. We have observed substantial anti-proliferative potentials against a lung cancer cell lines after 72 hours of treatment with an increasing dosage of a chosen phenolic fraction of CAN and LEX. Whereas, both of the extracted phenolic fractions were non-toxic to human PBMCs. It is possible that the chosen plant fraction preferentially inhibits the proliferative potentials of lung cancer cells. Targeted detection of tumour cells is crucial for increasing the cytotoxic drug's therapeutic efficiency while lessening the drug's damaging effects on nearby healthy tissues.

The lung cancer cells were undergoing apoptosis or necrosis typically exhibits a set of recognizable morphological hallmarks that can be used to positively identify the process. These hallmarks include a membrane rupture, reduction in cell and nuclear volume, chromatin condensation, DNA fragmentation, formation of membrane-bound vesicles and lipid accumulation that can be triggered by a number of different intracellular pathways. After exposure to our phenolic fractions, lung cancer cells showed conventional changes in morphologies while control cells had not undergone any morphological changes over the duration of the experiment. Microscopic and flowcytometric analysis of phenolics fraction treated cells confirms the lung cancer cell death either by apoptosis or autophagy.

We have found that the phenolic fraction of CAN and LEX induced a dose-dependent increase in intracellular ROS level and MMP in comparison to control in lung cancer cell lines used in the study. Hence we can correlate the cellular stress induced after exposure of the phenolics fraction might lead to ROS and MMP–mediated cell death either by apoptotic or autophagic pathways. Interestingly, oxidative stress induced by the plant phenolic fraction leads to lipid accumulation in lung cancer cells which directly correlates to and autophagic cell death. The clonogenicity and cell migratory property of the lung cancer cell lines were significantly inhibited after exposure of the phenolic fractions suggesting the effectiveness of the selected plant phenolics used in the study. In comparison of known drug, Cisplatin, we have observed significant arrest in cell cycle of lung cancer cells after exposure to free and bound phenolics of CAN and LEX for 48 hours.

The study of hepatological, nephrological and hematological parameters suggest that the free phenolics of CAN and LEX were not toxic to Balb/C mice. The tumor burden and size is strongly inhibited in A549 induced cancer in athymic nude mice after treating with the free phenolic fractions.

Collectively, our findings support the conclusion that phenolic fractions isolated from the leaves of *Etlingera linguiformis* (CAN) and *Smilax ovalifolia* (LEX) inhibit human lung cancer cell proliferation by causing cell. A major breakthrough in the novel drug discovery of therapeutic and preventative aspects of cancer management could be made through the identification, isolation, and investigation of active molecules present in the leaves of *Etlingera linguiformis* (CAN) and *Smilax ovalifolia* (LEX) for their anticancer efficacy. It is crucial for elucidating the precise molecular mechanisms, which could lead to a breakthrough in the novel drug discovery of therapeutic and preventive aspects of cancer management. Therefore, it is necessary to investigate the untapped potential of plants of ethnobotanical relevance in the battle against cancer-like disorders, a topic that has remained obscure for several years.